Doctoral Thesis

Cortical control of subthalamic activity through the hyperdirect and indirect pathways in monkeys

Polyakova, Zlata

SOKENDAI (The Graduate University for Advanced Studies)

School of Life Science

Department of Physiological Sciences

2019

Contents

Abstract

The subthalamic nucleus (STN) plays a key role in the control of voluntary movements and basal ganglia (BG) disorders, such as Parkinson's disease and hemiballismus. It is known that lesion, chemical blockade or deep brain stimulation (DBS) of the STN is an effective treatment of movement disorders. The STN receives glutamatergic inputs directly from the cerebral cortex and gamma-aminobutyric acid mediated (GABAergic) inputs from the external segment of the globus pallidus (GPe), which are mediated by the cortico-STN *hyperdiret* and cortico-striato-GPe-STN *indirect* pathways, respectively. Then, the STN drives the internal segment of the globus pallidus, the output nucleus of the BG. Thus, it is important to clarify how STN neuronal activity is controlled by these inputs.

In the first part of the study, I investigated the origin of each component of the biphasic response in the STN induced by cortical stimulation in awake monkeys (*Macaca fuscata*, *n = 2*). In the present study, I considered two hypothetical options for the formation of the STN biphasic response evoked by cortical stimulation. 1) Early and late excitations are mediated by the *hyperdirect* and *indirect* pathways, respectively. In that case, the origin of early excitation is excitatory input from the cortex and the origin of late excitation is disinhibition from the GPe. 2) Cortically induced long excitation is intervened by the inhibition from the GPe through Cx-STN-GPe-STN transmission. In order to clarify this issue, I recorded neuronal activity in the STN combined with electrical stimulation of the motor cortices: primary motor cortex (MI) and supplementary motor area (SMA). Cortical stimulation induced early excitation and following late excitation in STN neurons. In order to examine the origin of these biphasic responses, neuronal

responses were compared before and after drug application into the basal ganglia. Local application of glutamatergic antagonists, especially N-methyl-D-aspartate (NMDA) receptor antagonist, into the vicinity of recorded STN neurons, diminished the early excitation among biphasic responses. Blockade of the striatum by local injection of muscimol, $GABA_A$ receptor agonist and blockade of the GPe by local injection of muscimol diminished late excitation. Blockade of the striato-GPe transmission by local injection of gabazine, $GABA_A$ receptor antagonist, into the GPe also abolished late excitation. These results suggest that cortically induced early and late excitation in STN neurons are mediated by *the hyperdirect* and *indirect* pathways, respectively, and that cortical inputs to the STN are mainly mediated by NMDA receptors.

In the second part of the study, I examined the degree to which STN neuronal activity is involved specifically in voluntary movement control and their origins as described above. *Monkey S* was trained to perform goal-directed reaching task with delay that includes "Go/Stop/NoGo" types of trials. In "Go" trials after the triggering signal, the monkey was required to perform reaching movements to the target, which was indicated by an instruction signal. In "Stop" trials, same types of instruction signals were presented as in "Go" trials, however, the triggering signal was different and indicated stopping of action. In "NoGo" trials, from the beginning the monkey was informed by instruction signal that movement performance is not required. This task paradigm combined with cortical stimulation and manipulation of inputs by local drugs application into the STN allows us to investigate cortical control of STN activity during motor performance. The results showed that MI-receiving region in the STN is involved in both motor execution and cancellation. Task-related STN activity was also controlled through direct glutamatergic and indirect GABAergic inputs from the cortex. Stop-related activity

was mainly transmitted through the *hyperdirect* pathway that caused facilitation in the STN, while the role of the *indirect* pathway was minor. I revealed the direction selective (DS) activity in both "Go" and "Stop" trials, suggesting that some neurons with stop-related activity involved in a specific stop, while other neurons participated in a global stop.

The functions and neural dynamics of the STN in voluntary movement control are still under debates nowadays. In the present study, I demonstrated the influence of the *hyperdirect* pathway on early excitation and the *indirect* pathways on late excitation of the STN biphasic response induced by cortical stimulation. I also discussed the role of glutamatergic and GABAergic inputs to the STN in motor control. I would like to suggest based on the results that the STN plays a specific role in motor execution and cancellation, which is regulated by inputs from both *hyperdirect* and *indirect* pathways.

Introduction

The subthalamic nucleus (STN) plays a critical role in the control of voluntary movements as the driving force of the basal ganglia. STN neurons change their activity in relation to limb and eye movements (Delong et al. 1985, Hikosaka et al. 2000). Recent studies highlighted STN activity specific to inhibiting/cancelling movements or changing task (Isoda et al. 2008, Schmidt et al. 2013, Pasquereau et al. 2017). Lesion or chemical blockade of the STN reduced firing rate of GPe/GPi neurons and interferes normal voluntary movements by inducing involuntary movements, hemiballismus (Whittier et al. 1949, Carpenter et al. 1950, Hamada et al. 1992, Nambu et al. 2000). Abnormal activity of STN neurons, such as firing rate and pattern changes, has been reported in various movement disorders, such as Parkinson's disease (PD) (Bergman et al. 1994, Hassani et al. 1996, Galvan et al. 2008) and dyskinesia (Wichmann et al. 1994, Rodriguez-Oroz et al. 2001, Hanson et al. 2012). Moreover, lesions or chronic high-frequency stimulation in the STN ameliorate PD symptoms (Bergman et al. 1990, Aziz et al. 1991, Pollak et al. 1993, Benabid et al. 1994, Limousin et al. 1995). Therefore, it is important how steady state and phasic STN activity is controlled by afferent inputs to the STN.

The STN is an input station as well as a relay nucleus of the basal ganglia. It receives somatotopically organized glutamatergic inputs directly from the frontal cortex, forming the cortico-STN *hyperdirect* pathway (Monakow et al. 1978, Nambu et al. 1996, Nambu et al. 2000, Nambu et al. 2002). It also receives gamma-aminobutyric acid (GABA)ergic inputs from the external segment of the globus pallidus (GPe) as a relay nucleus in the striato-GPe-STN *indirect* pathway (Alexander et al. 1990). The STN finally

projects to the GPe and the internal segment of the globus pallidus (GPi), an output station of the basal ganglia, and control their activity (Jaeger et al. 2011).

The STN is composed of glutamatergic neurons which spontaneously fire at mid-frequency (20-40 Hz). Cortical stimulation induced biphasic response, which is composed of early excitation and late excitation, interposed by a short gap (Nambu et al. 2000). There are two possibilities of the origin of biphasic response in the STN induced by cortical stimulation. 1) Early and late excitations are mediated by the *hyperdirect* and *indirect* pathways, respectively, which was shown in anesthetized rats experiments (Kitai et al. 1981, Rouzaire-Dubois et al. 1987, Fujimoto et al. 1993, Maurice et al. 1998). 2) Cortically induced long excitation is intervened by the inhibition from the GPe through Cx-STN-GPe-STN transmission. The rebound excitation after the inhibition might contribute to late excitation. The origin of that biphasic response is still not clear in monkeys. The first goal of the present study is to investigate the origin of each component of the biphasic response in the STN induced by cortical stimulation in awake monkeys. The second goal of the present study is to examine the control mechanism of STN spontaneous activity through the *hyperdirect* and *indirect* pathways: the former inputs to the STN are glutamatergic and the latter inputs are GABAergic.

In the present study, I also made an attempt to clarify neuronal substrates of voluntary movement control. The classical model of BG (DeLong 1990, Mink 1996) suggests that STN implements excitatory influence on the basal ganglia output nuclei, which inhibit the thalamus and the cortex. Studies of the STN in animals and humans demonstrated its activation during movement inhibition (Aron et al. 2006, Ray et al. 2012, Schmidt et al. 2013, Bastin et al. 2014). The STN activity was reported to play a key role

in action suppression (Frank 2006, Li et al. 2008, Sharp et al. 2010, Fife et al. 2017, Pasquereau et al. 2017). The signals through the *hyperdirect* and *indirect* BG pathways are considered to be able to block activity responsible for motor initiation that transmits through the direct pathway (Mink 1996, Nambu et al. 2002, Nambu 2004). Moreover, there is evidence that STN activity is modulated in relation to the motor planning and voluntary limb movements (Alexander et al. 1990, Fischer et al. 2017, Zavala et al. 2017). Thus, I hypothesize that a subdivision of STN neurons might be involved in motor program execution and cancellation. In this study, I made an attempt to clarify the functions of the STN in the information processing and integration during motor task performance.

In order to reveal the specific role of the STN in movement and the influence of each pathway on the STN movement-related activity, I used combination of "Go/Stop/NoGo" tasks (Verbruggen et al. 2008, Schall et al. 2012, Pasquereau et al. 2017), which are typically used to study neuronal activity in motor performance and stop conditions. Here I hypothesize that STN functions are implemented differently by the cortico-STN *hyperdirect* and cortico-striato-GPe-STN *indirect* inputs based on behavioral contexts: the "Go" process may be initiated through both the *hyperdirect* and *indirect* pathways, while "Stop" process, which requires quick processing, may involve the *hyperdirect* pathway. However, there is no direct evidence regarding this question. Thus, the third goal of the present study is to clarify the degree to which STN neuronal activity is involved specifically in voluntary movement control and inputs to the STN activity.

Materials & Methods

Animals

The experimental protocols were approved by the Institutional Animal Care and Use Committee, and all experiments were performed in accordance with the guidelines of the National Institutes of Health *Guide for the Care and Use of Laboratory Animals*. Three female Japanese monkeys (*Macaca fuscata, Monkey K8, K9, and S*), weighing 5.8, 5.5 and 6.2 kg, were used in this study. *Monkey K8, K9* were used for simulation study, and *Monkey S* for behavioral study. The animal was housed in individual primate cages and had ad libitum access to food and water. Each monkey was trained to sit in a primate chair quietly.

Behavioral task

In the present experiment, I trained *Monkey S* to perform goal-directed reaching task with delay using its right upper limb in order to investigate the role of the STN in voluntary movement control. The task was combined two paradigms: the “Stop” signal task and the “Go/NoGo” task. "Stop" and "NoGo" tasks targeted different aspects of movement suppression, such as sudden cancellation and steady inhibition.

In the present task, I used a touch panel with three slots (Left, Center, Right; height, 18 mm, width, 6 mm, and depth, 11 mm), which were aligned horizontally with 10 cm intervals. In the bottom of each slot a two-color (green and red) light-emitting diode (LED) was installed. The touch panel was placed at distance of 30 cm in front of a monkey. The task includes three types of trials: “Go”, “Stop” and “NoGo” (Figure 1). Each trial was initiated after the monkey placed its hand at the resting position that was located below the touch panel for at least 1500 ms.

In “Go” trials (Figure 1), one of three LEDs was lit with red color for 150 ms as an instruction signal (S1). After that, a random delay period (550-1800 ms) was introduced. The monkey was required to keep its hand at the resting position during the S1 and delay periods. After a delay period, all three LEDs were lit with green color for 1200 ms as a triggering signal (S2). Within S2 presentation monkey was required to put its index finger inside the slot that has been instructed by S1. If the monkey reach the correct target within S2 presentation, it was rewarded (RW) with sweetened water. If the monkey released its hand before S2 presentation, reached the wrong slot, or reached the target after 1200 ms, the trial with the same task conditions was repeated. The timings of hand release (HR) from the resting position and finger in (FI) the slot were detected by infrared photoelectric sensors (Keyence, Japan), installed in the resting position and slots on the touch panel.

In “Stop” trials (Figure 1), S1 was similarly presented to “Go” trials. After the delay, all three LEDs were lit with red color as S2. The monkey was required to cancel movements. If monkey kept its hand at the resting position during the entire task period, it was rewarded.

In “NoGo” trials (Figure 1), all three LEDs were lit simultaneously with red color as S1. After a random delay period, all three LEDs were lit with green color as S2. In that case, the monkey was required to keep the hand at the resting position during the entire task period to get reward.

“Go”, “Stop” and “NoGo” trials were randomly presented with a probability of 60, 30, and 10% respectively. Left, Center and Right targets were also randomly presented with equal probability. The task was controlled by LabVIEW Real Time software (National Instruments) and a computer.

The monkey was trained to perform the task with short (250-280 ms) reaction times and high successful rate (> 90%) in all trial conditions.

Surgery

After the chair training (*Monkeys K8 and K9*) and task training (*Monkey S*), monkeys received aseptic surgical operation to fix their head painlessly in a stereotaxic frame attached to a monkey chair (for details, see (Nambu et al. 2000, Nambu et al. 2002)). Briefly, under general anesthesia with thiopental sodium (25 mg/kg body wt, iv) after ketamine hydrochloride (10 mg/kg, im) and xylazine hydrochloride (1-2 mg/kg, im), or with propofol (6-9 μg/ml, target blood concentration) with fentanyl (2-5 μg/kg, im) after ketamine hydrochloride (10 mg/kg, im) and xylazine hydrochloride (1-2 mg/kg, im), the monkey head was fixed in stereotaxic apparatus, the skull was widely exposed and covered with transparent acrylic resin (Unifast II; GC Corporation), and two polyether ether ketone (PEEK) or stainless tubes were mounted for head fixation. Antibiotics (amikacin sulfate) and analgesics (ketoprofen) were administrated post-surgically. After full recovery from the above operation, the skull over the primary motor cortex (MI) and supplementary motor area (SMA) was removed under anesthesia with ketamine hydrochloride (10 mg/kg, im) and xylazine hydrochloride (1-2 mg/kg, im). Electrophysiological mapping was performed and the forelimb regions of the MI and SMA were identified by recording neuronal activity in response to somatosensory stimuli and observing body part movements evoked by intracortical microstimulation (for details, see (Nambu et al. 2000, Nambu et al. 2002)). After mapping, two pairs of bipolar stimulating electrodes (enamel-coated stainless steel wires, 200 μm diameter; 2 mm intertip distance) were implanted chronically into the distal and proximal forearm regions

of the MI, and one pair into the forearm region of the SMA (Figure 2A). Exposed areas were covered with the transparent acrylic resin except two areas (10-15 mm diameter) for access to the putamen, GPe, and STN. Two rectangular plastic chambers covering each craniotomy were fixed onto the skull with acrylic resin. Animals were administered antibiotics, steroids (dexamethasone), and analgesics after the surgical procedures. Recordings of neuronal activity were started after full recovery from the second surgery.

Recording STN neuronal activity

Recording of STN neuronal activity was performed two or three days per week for several months. During the experimental session, the monkey was seated in a primate chair with head fixed in the frame, leaving body and limbs free to move. Recordings were performed while the monkey was awake. First, the location and borders of the STN were defined based on the single-unit extracellular recordings. Using a hydraulic Microdrive, a glass-coated Elgiloy microelectrode (0.7–1.5 MΩ at 1 kHz) was penetrated vertically into the STN through dura mater with a local application of lidocaine. The neuronal activity of STN recorded from the microelectrode was amplified (x 10,000), filtered (100 Hz to 2 kHz). The unitary activity of STN neurons was isolated, converted into digital data with a homemade time-amplitude-window discriminator, and sampled using LabVIEW software (National Instruments) and a computer for online data analysis. The unitary activity and converted digital data were also stored on videotapes using a PCM recorder. The monkey's arousal level was maintained during recording by monitoring the spontaneous firing rate and patterns of activity of STN neurons. Peri-stimulus time histograms (PSTHs; 1 ms bin, summed for 100 stimulus trials) were constructed to examine responses to electrical stimulation through the electrodes implanted in the MI

and SMA (bipolar stimulation, 300 μs duration, single pulse, strength of 0.5-0.7 mA and interval of 1.4 s). STN neurons can be identified by mid-frequency (20 - 40 Hz) firings and responses to passive joint movements. The most reliable criterion is the pattern of the responses to cortical stimulation: the response pattern of STN neurons is early and late excitations intervened by a short gap (Nambu et al. 2000). The STN can be easily discriminated from surrounding structures, such as zona incerta and lateral hypothalamus by using these criteria.

In *Monkey S*, neuronal activity during performance was also recorded and stored in computer.

Drug injection in the vicinity of recorded STN neurons

Single-unit recordings of STN neurons in combination with local applications of drugs were performed with an electrode assembly consisting of a glass-coated Elgiloy microelectrode (0.7–1.5 MΩ at 1 kHz) for unit recording and two silica tubes (OD, 150 μm; ID, 75 μm; Polymicro Technologies Inc, Phoenix, AZ, USA) for drug delivery (Figure 2B) (Kita et al. 2004, Tachibana et al. 2008). The silica tubes were connected to two 25-μl Hamilton microsyringes, which contained two of the following drugs dissolved in saline: 1) the *N*-methyl-$_D$-aspartate (NMDA) receptor antagonist, ±3-(2-carboxypiperazin-4-yl)propyl-1-phosphonic acid (CPP, 1 mM, Sigma, St Louis, MO, USA); 2) the alpha-amino-3-hydroxy-5-methylisoxazole-4-propionic acid (AMPA)/kainate receptor antagonist, 1, 2, 3, 4-tetrahydro-6-nitro-2, 3-dioxo-benzo[f]quinoxaline-7-sulfonamide disodium (NBQX, 1 mM, Sigma); 3) a mixture of CPP (1-2 mM) and NBQX (1-2 mM); 4) the $GABA_A$ receptor antagonist, gabazine (SR95531, 1 mM, Sigma). Using a hydraulic microdrive, the electrode assembly was

penetrated vertically into the STN through a small incision of dura made with a local application of lidocaine. The neuronal activity of STN neurons was recorded, and PSTHs were constructed to examine responses to cortical stimulation as described above. When STN neurons responded to MI and/or SMA stimulation, a total volume of 0.2 - 0.6 µl of each drug was injected at a rate of 0.03-0.05 µl/min by advancing plungers with computer control (Nihon Kohden, XF-320-J or UltraMicroPump III, WPI). This amount of drugs is expected affect areas approximately 1mm from the injection site as described elsewhere (Kita et al. 2004). As the drug effects became maximum 10-15 min after injection and decayed very slowly, the special attention was paid to this period and PSTHs were constructed. Digitized spontaneous activity was also recorded for 50 s before and after drug injections, and autocorrelograms (0.5 ms bin width) were constructed. Injection sites were located at least 1 mm apart because the effective radius of the drugs was estimated to be ~1 mm (Kita et al. 2004). I also confirmed that injections of saline alone did not alter the spontaneous firing rates and patterns and the cortically induced responses of STN neurons.

Drug injection into the putamen or GPe

This experiment was done in *Monkey K8* and *K9*. First, forelimb region of the putamen and GPe were mapped by recording neuronal activity. Using a hydraulic microdrive, a glass-coated Elgiloy microelectrode (0.7–1.0 MΩ at 1 kHz) was penetrated obliquely (45 degrees from vertical in the frontal plane) into the putamen or GPe through dura mater with a local application of lidocaine. The forelimb region of the putamen or GPe was identified by firing patterns, passive joint movements, and responses to cortical stimulation (Nambu et al. 2000, Nambu et al. 2002, Kita et al. 2004). Typical response

patterns are excitation in the putamen and triphasic response composed early excitation, inhibition and late excitation in the GPe.

The method for drug injection into the putamen or GPe was the same as described elsewhere (Tachibana et al. 2008). A Teflon-coated tungsten wire (bare diameter, 50 μm) was attached to the 31-gauge needle (OD, 250 μm) of a 10-μl Hamilton microsyringe, and they were covered by polyamide tubing except for the tip (1 mm). A tungsten wire was used not only as a recording electrode but also as bipolar stimulating electrodes together with the syringe needle (0.7 mm inter tip distance). A Hamilton microsyringe contained one of the following drugs dissolved in saline, muscimol ($GABA_A$ receptor agonist, 0.5 mM, Sigma), NBQX (10 mM) and gabazine (10 mM). Using a hydraulic microdrive, the needle was penetrated obliquely (45 degrees from vertical in the frontal plane) into the putamen or GPe through a small incision of dura made with a local application of lidocaine. The orifice of the microsyringe was set at the center in the forelimb regions of the putamen or GPe by recording neuronal activity through a tungsten wire as described above. For STN recording, a glass-coated Elgiloy microelectrode (0.7–1.5 MΩ at 1 kHz) was penetrated vertically using a hydraulic microdrive, and neuronal activity was isolated. When STN neuron responded to cortical stimulation, the neuronal response to the putamen or GPe stimulation (bipolar stimulation, 300 μs duration, single pulse, strength of 0.1 - 0.7 mA, sometimes up to 1.0 mA and interval of 1.4 s) was examined, and a total volume of 1.0 - 4.0 μl of the drug was injected into the putamen or GPe in the following combination: muscimol injection to the striatum to block striatal activity, muscimol injection to the GPe to block GPe activity, gabazine injection into the GPe to block putaminal GPe GABAergic neurotransmission. Cortical stimulation induced

responses in certain areas of the putamen and GPe, and of 1.0 - 4.0 µl of the drug is needed to cover responsible areas of the putamen and GPe.

EMG recording

Electromyograms (EMGs) were recorded two times for *Monkey S* using surface electrodes from the following muscles: wrist extensor, wrist flexor, biceps brachii, triceps brachii, trapezius, and deltoid. EMG signals were amplified (x 2,000), filtered (100-1000Hz), rectified, and sorted on a computer.

Data analysis of stimulation study

Neuronal responses to the cortical stimulation and spontaneous firing rates and patterns were analyzed using Igor Pro software version 6.3.7.2 (WaveMetrics) and compared before and after drug injection into the STN, putamen or GPe. Different drugs were injected into the STN in a different order (Table 1). Responses of STN neurons induced by cortical stimulation were evaluated based on PSTHs. The mean and standard deviation (SD) of the discharge rate during the 100 ms period preceding the onset of stimulation were calculated for each PSTH and considered as the baseline discharge rate. Changes in neuronal activity in response to cortical stimulation (i.e., excitation and inhibition) were judged to be significant if the firing rate during at least two consecutive bins (2 ms) reached the statistical level of mean ± 1.65 SD (corresponding to $p < 0.05$, one-tailed *t*-test) (Iwamuro et al. 2017). The maximum effect of drugs injections was observed in 10-15 min and decayed very slowly, thus the analysis of PSTHs was performed during this period. The amplitude and duration of cortically evoked responses in the STN were analyzed before and after drug injection into the STN, putamen or GPe. Duration of excitation or inhibition was defined as the period of significant response (≥

mean + 1.65 SD or ≤ mean – 1.65SD). Amplitude was calculated as a number of spikes during the significant response minus that of the baseline discharge (mean) (area of the significant response over or below the mean). Population PSTHs of STN neurons were constructed by averaging PSTHs of each neuron and smoothing with a Gaussian filter (σ = 10 ms) for each case of drugs injections, and displayed with ± SD.

Spontaneous firing rates and patterns were analyzed using continuous digitized recordings for 50 s. The following parameters were calculated: mean and SD of firing rates, mean, SD, and mode of inter-spike intervals (ISIs), burst index (BI) defined as the ratio of the mean of ISIs and the mode of ISIs, and coefficient of variation (CV) defined as the ratio of the SD of ISIs and the mean of ISIs. Spontaneous firing patterns were also analyzed by calculating autocorrelograms (0.5 ms bin width, for 50 s). The mean and SD of values between 900 and 1000 ms (200 bins), that was far enough from *time 0*, were calculated as control values because of a flat autocorrelogram during this period. Peaks and troughs of the autocorrelation were judged to be significant if the coefficient during at least two consecutive bins (1 ms) exceeded the confidence limits ($p< 0.005$, one-tailed *t*-test; (Tachibana et al. 2008)). The regularity of firing was assessed by the existence of multiple peaks and their height in the aotucorrelograms. Adequate and stable spike isolation during a recording session was confirmed by constructing ISIs histograms: absence of ISIs < 2 ms (the refractory period).

Paired, one-tailed *t*-tests were used to compare parameters before and after drug injections. Bonferroni tests were used to compare parameters of MI- and SMA-recipient neurons. $P < 0.05$ was considered significant.

Data analysis of behavioral study

The analysis of neuronal activity during the goal-directed reaching task with delay was performed to reveal the difference of the activity relative to different types of trials, task events, and targets before and after local drugs injections in the vicinity of recorded STN neurons. First, I examined response to cortical stimulation, and recorded activity of STN neurons, which receive cortical inputs from the forelimb area of the MI, during task performance.

In the case of raster plots and population histograms in the behavioral task, neuronal activity was aligned separately according to the instruction signal (S1), triggering signal (S2), hand release from the resting position (HR), finger in the slot (FI) and reward (RW) timings for all types of trials, i.e., Go (Left, Center, Right), Stop (Left, Center, Right) and NoGo trials. Spike-density functions (SDFs) were calculated by smoothing the averaged activity with a Gaussian filter (σ = 10 ms). GABAergic and glutamatergic components were calculated as subtraction of SDFs for successful trials before and after drugs injections:

GABAergic component = (SDF before gabazine) – (SDF after gabazine);

Glutamatergic component = (SDF before NBQX+CPP) – (SDF after NBQX+CPP).

In order to detect target- and event-related changes in SDFs and component (GABAergic, glutamatergic), the mean ± SD during 1000 ms preceding S1 were calculated as the baseline. If a neuron demonstrated delay related changes (S1-S2 time period), which reached a significant level ($p < 0.001$, one-tailed *t*-test) within 300 ms interval before S2, the mean ± SD during the 500 ms period before S2 were used as the

baseline. The amplitudes of SDFs and component functions relative to task events were calculated for the following time intervals: Delay period, 700 ms after S1; S2, 200 ms before and after S2; HR, 300 ms before and 400 ms after HR; FI, 300 ms before and 300 ms after FI; RW, 200 ms before and 200 ms after RW. The following calculations were performed for the functions aligned separately to each corresponding task event. When changes exceed the significant level of the mean ± 3.09 SD ($p < 0.001$, one-tailed *t*-test) for at least 10 ms for SDFs and 3 ms for component functions, it was considered as significant activity change. The start point was defined as the time when the amplitude exceeded mean ± 1.65 SD ($p < 0.05$, one-tailed *t*-test). The end point was defined as the time when the amplitude dropped below the significant level $p < 0.05$. The baseline activity was subtracted for the amplitude calculation and averaged by the number of trials performed.

The latency of significant changes was calculated with settings different from the mentioned above in order to detect the timing of neuronal activity changes that related to the actual movement. The latency was defined as the time from the S2 presentation to the first amplitude of the largest neuronal response among three targets, where mean ± 3.09 SD ($p < 0.001$, one-tailed t-test) was calculated for the 200 ms period before S2.

Delay-, S2-, HR-, and FI-related activity were modulated by target directions. Directional selectivity (DS) of a neuron in each event was defined as:

$$DS = 1 - (|A_{med}| + |A_{min}|)/(|A_{max}| * 2),$$

where $|A_{max}|$, $|A_{med}|$, and $|A_{min}|$ are the absolute values of maximum, medium and minimum amplitudes among three targets (Left, Center, Right), respectively (Takara et al. 2011). DS varies between 0 and 1. DS = 0 means the same amplitude among three

targets. DSs were calculated for both SDFs and component functions (GABAergic, glutamatergic). For each neuron, SDFs or component functions with the largest changes among three targets were selected for calculation of population activity.

I classified recorded STN neurons based on the components: 1) Positive or negative changes of components, and 2) Presence or absence of the buildup activity during delay periods. I further classified STN neurons to following four groups based on the first criteria: I) Negative GABAergic and positive glutamatergic components; II) Positive GABAergic and positive glutamatergic components; III) Positive GABAergic and negative glutamatergic components; and IV) Negative GABAergic and negative glutamatergic components. According to the second criteria I picked up neurons with buildup activity during the delay period after S1 event for each component (GABAergic and glutamatergic, separately). DSs of each component at each task events were calculated.

EMG activity was analyzed using similar methods as applied for neuronal activity in task performance. EMG activity was aligned at task events such as, S1, S2, HR, and FI. The mean value and SD of the activity were calculated during 1000 ms before S1 presentation. EMG activity was considered as significant activity changes when EMG activity exceed the significant level of the mean + 3.09 SD ($p < 0.001$, one-tailed *t*-test) for at least 10 ms.

Histology

At the end of experiments, the recording and drug injection sites were marked by current injections (cathodal DC current of 20 μA for 30 s). Monkeys were deeply anesthetized with sodium pentobarbital (50 mg/kg, iv) and perfused transcardially with

0.1 M phosphate-buffered saline (pH 7.3), followed by 10% formalin in 0.1 M phosphate buffer (PB), and the same fresh buffer containing 10% sucrose and then 30% sucrose. The brains were removed and kept in 0.1 M PB containing 30% sucrose at 4°C, and then cut serially into 60-µm-thick frontal sections on a freezing microtome. These sections were mounted onto gelatin-coated glass slides and stained with 1% Neutral Red. The recording and drug injection sites were reconstructed according to the lesions made by current injections and the traces of the electrode tracks.

Results

Overview of recorded STN neurons

A total of 158 STN neurons (79 neurons in *Monkey K8*; 79 neurons in *Monkey K9*) were recorded, and drug injections were performed in 91 STN neurons. Among them, 70 STN neurons were selected based on isolation criteria and presence of significant biphasic responses to cortical stimulation (for details, see *Materials & Methods*) and analyzed in combination with drug injections into the STN (33 neurons), putamen (15 neurons) or GPe (22 neurons) (Table 1). The spontaneous firing rates of these STN neurons were 34.4 ± 16.9 Hz (mean ± SD). Cortical stimulation induced a biphasic response composed of early and late excitations, which were intervened by a short "gap" (Figure 3) in STN neurons, and they were classified into 35 MI-recipient (50%, responded to MI-, but not to SMA-stimulation), 24 SMA-recipient (34%; responded to SMA-, but not to MI-stimulation), and 11 MI+SMA-recipient (16%; responded to both MI- and SMA-stimulation) STN neurons. The latency of each component is compared and agrees with data reported previously (Nambu et al. 2000, Iwamuro et al. 2017). The latencies, durations, and amplitudes of the early excitation, gap, and, late excitations were compared between MI- and SMA-stimulation (Table 2). Latencies evoked by MI-stimulation were significantly shorter than those evoked by the SMA-stimulation (early excitation, $F(1,68) = 56.52$, $p = 1.6 \times 10^{-10}$, late excitations, $F(1,68) = 10.67$, $p = 1.7 \times 10^{-3}$, Bonferroni test), and these data agree with the data reported previously (Nambu et al. 2000, Iwamuro et al. 2017). The duration of the gap was longer ($F(1,68) = 14$, $p = 0.4 \times 10^{-3}$, Bonferroni test) and the amplitude of early excitation was smaller ($F(1,68) = 8.07$, $p = 5.9 \times 10^{-3}$, Bonferroni test) in SMA-stimulation than in MI stimulation. On the other hand, durations of the excitations were comparable between MI- and SMA-stimulation, and thus

durations and amplitudes obtained by MI and SMA stimulation were grouped together and analyzed in the following drug injection experiments. In 70% of cases, these biphasic responses were followed by a long inhibition (latency, 40-70 ms, duration 40-200 ms).

Drug injection in the vicinity of recorded STN neurons

CPP, NBQX and/or gabazine were applied in the vicinity of 36 STN neurons in various combinations and sequence (Table 1). The mixture of NBQX and CPP (NBQX + CPP) was applied in the vicinity of 15 STN neurons to examine the contribution of the glutamatergic inputs through the ionotropic receptors (Figure 4). The typical example was shown in Figure 5A1, and the early and late excitation were suppressed after CPP + NBQX injection. Quantitative analyses showed that the amplitude (to 42.4%; $p = 1.7 \times 10^{-3}$, one-tailed paired *t*-test) and duration (to 26.4%; $p = 0.024$) of early excitation, and the amplitude (to 38%; $p = 0.035$) of late excitation evoked by cortical stimulation were significantly decreased after NBQX + CPP injection (Figure 5A2; Table 3). The duration of a gap between early and late excitation was increased (to 84%; $p = 0.02$, paired, one-tailed *t*-test; Table 3), and might partly contribute to the attenuation of early and late excitation. These changes were also observed in population PSTHs (Figure 5A3). These results suggest that early and late excitation is related to glutamatergic inputs.

Next, I examined whether NBQX (AMPA/kainite receptor blocker) or CPP (NMDA receptor blocker) effectively suppress early and late excitation, I applied separately NBQX and CPP in the vicinity of STN neurons (Table 1). NBQX was applied in the vicinity of 8 STN neurons as exemplified in Figure 5B1. The amplitude of late excitation was significantly decreased (to 19.5%; $p = 0.024$, one-tailed paired *t*-test) after NBQX injection, but no changes were observed in early excitation (Figure 5B2; Table 3).

CPP was additionally applied in the vicinity of 6 STN neurons as exemplified in Figure 5B1. The amplitude of cortically evoked early excitation in the STN was decreased (to 57.2%; $p = 6.5 \times 10^{-3}$, one-tailed paired *t*-test) after CPP injection into the STN (Figure 5B2; Table 3). These changes were also observed in population PSTHs (Figure 5B3). Drugs were injected in the reverse order (CPP, then NBQX) only one time, and CPP suppressed specifically early excitation (data not shown). These results suggest that the NMDA receptors have a stronger effect on the early excitation evoked by cortical stimulation than AMPA/kainite receptors, which mainly contributed to late excitation

Further gabazine injection after NBQX + CPP injection was performed in the vicinity of 5 STN neurons (Figure 5A1). The amplitude of late excitation, but not the duration, was significantly decreased (to 62.1%; $p = 0.028$, one-tailed paired *t*-test) after gabazine injection (Figure 5A2, 3; Table 3), and the gap was not changed. When gabazine was first injected before NBQX + CPP injection (reversed order; Figure 5C1), no significant changes were detected for early excitation, gap, and late excitation (Figure 5C1, 2, 3; Table 3). Additional NBQX + CPP injection decreased both early (Figure 5C2, 3; Table 3) and late excitation. These data suggest that the late excitation in the STN evoked by cortical stimulation may be related to GABAergic inputs. On the other hand, the gap was not induced by GABAergic input.

I also examined the effects of local drug injection on the spontaneous firing rates and patterns (Table 4, Figure 6). After NBQX + CPP injection, the spontaneous firing rate was decreased (to 16%; $p = 0.024$, one-tailed paired *t*-test; Table 4), and was not changed after additional gabazine (Table 4). The spontaneous firing rate was not changed by separate injections of NBQX or CPP, and was significantly decreased ($p = 0.017$, one-

tailed paired *t*-test) only when the injection of both drugs. After gabazine injection without NBQX and CPP, the spontaneous firing rates were increased (to 26.5%; p = 0.017, one-tailed paired, *t*-test), but were not changed after additional injection of NBQX and CPP (Table 4). These results suggest that spontaneous firing rates were continuously controlled by AMPA/kinate and NMDA glutamatergic and GABAergic inputs. There were no significant changes in BI and CV of STN spontaneous neuronal activity, except for the case of CV increase (to 20.3%; p = 0.008, paired, one-tailed *t*-test) after further gabazine injection in addition to NBQX+CPP injection (Table 4). No significant changes of spontaneous firing patterns were observed after local drug injection in autocorrelograms (Figure 6A) except the following cases: bursts and pauses in 3 STN neurons (21%; Figure 6B) and oscillations in 2 STN neurons (14%; Figure 6D; The oscillatory periods were around 10 ms) after NBQX + CPP injection, and oscillations in 2 STN neurons (22%; Figure 6C; around 9 ms) after gabazine injection.

Drug injection into the putamen

Above experiments of local drug injection into the STN suggest that cortically evoked late excitation is related to GABAergic inputs, which is mediated by the striato-GPe-STN indirect pathway. To examine this possibility, I blocked the striatal activity by injecting muscimol into the putamen (Figure 4, Figure 7A). Cortical stimulation induced early and late excitation. Muscimol injection into the putamen diminished late excitation (Figure 7A1). The amplitude (to 73.5%; $p = 0.01$, one-tailed paired *t*-test) and duration (to 50.3%; $p = 0.75 \times 10^{-3}$, one-tailed paired *t*-test) of cortically evoked late excitation in the STN were significantly decreased after muscimol injection into the putamen (Figure 7A2; Table 5), while those of early excitation remained unchanged. Population PSTHs

also confirmed that late excitation was diminished after muscimol injection into the putamen while early excitation remained unchanged (Figure 7A3). The spontaneous firing rates and patterns of STN neurons were also examined before and after drug injections. Firing rate, BI, and CV did not change after muscimol injection into the putamen. These data support the idea that the cortically evoked late excitation is mediated by the striato-GPe-STN indirect pathway.

Drug injection into the GPe

I further block the striato-GPe-STN indirect pathway by injection of muscimol or gabazine into the GPe (Figure 4, Figure 8). I first injected muscimol into the GPe (Figure 8A) to block GPe activity. Cortical stimulation induced early and late excitation in an STN neuron (Figure 8A1), and muscimol injection into the GPe decreased late excitation. The amplitude (to 70.5%; $p = 0.022$, one-tailed paired *t*-test) and duration (to 54.5%; $p = 0.028$, one-tailed paired *t*-test) of cortically evoked late excitation were significantly decreased after muscimol injection into the GPe (Figure 8A2; Table 6), while those of early excitation remained unchanged. These changes were also observed in population PSTHs (Figure 8A3). The spontaneous firing rates of STN neurons were significantly increased (to 26.7%; $p = 0.02$, one-tailed paired *t*-test). As a whole, no significant changes in BI and CV were revealed after muscimol injection into the GPe (Table 6). However, analyses of individual neurons showed pattern changes, such as bursts and pauses in 2 STN neurons (25%) and oscillations in 3 STN neurons (38%) (Figure 9A, B).

I also injected gabazine into the GPe (Figure 8B) to block the striato-GPe GABAergic neurotransmission. Cortical stimulation induced early and late excitation in an STN neuron (Figure 8B1), and gabazine injection into the GPe decreased late

excitation. The amplitude (to 82.6%; $p = 0.49 \times 10^{-3}$, one-tailed paired *t*-test) and duration (to 33.3%; $p = 6.4 \times 10^{-3}$) of cortically evoked late excitation in the STN were significantly decreased after gabazine injection into the GPe (Figure 8B2, C; Table 6), while those of early excitation remained unchanged. The gap was increased (to 53.3%; $p = 0.023$, one-tailed paired *t*-test) after gabazine injection into the GPe, and may partly contribute to attenuation of late excitation. The spontaneous firing rates of STN neurons were significantly decreased (to 63%; $p = 0.006$, one-tailed paired *t*-test) after gabazine injection into the GPe (Table 6). BI (to 352%; $p = 0.012$, paired, one-tailed *t*-test) and CV (to 45.5%; $p = 0.019$) were increased after gabazine injection into the GPe (Table 6). Bursts were increased in 3 STN neurons (33%) (Figure 9C).

The GPe also receives the glutamatergic inputs from the STN. Actually, cortical stimulation induces early excitation in the GPe through the cortico-STN-GPe glutamatergic projections, and the early excitation can be blocked local injection of gabazine into the GPe. Cortical stimulation induced early and late excitation in the STN in control state, and NBQX injection into the GPe did not change early and late excitations and duration of the gap between them (Figure 8C1, 2, 3; Table 6). These data suggested that the gap was not induced the cortically evoked early excitation. Spontaneous firing rates and patterns were not changed after NBQX injection into the GPe.

Locations of recorded STN neurons and drug injection sites in the putamen and GPe

Locations of recorded STN neurons were plotted in *Monkey K8* and *K9* based on the experiments, such as local drug injections into the STN (Figure 10A1, B1) and drug injections into the GPe or striatum (Figure 10A2, B2). The recorded STN neurons were found in the dorsal half of the STN, corresponding to the somatomotor region of the STN.

Drug injection sites in the putamen and GPe were also plotted (Figure 10A3, B3), and they were found in the dorso-ventral mid points in the GPe and putamen, also corresponding to the somatomotor region of the GPe and putamen, respectively.

Task-related activity in the control state

I recorded 115 STN neurons in *Monkey S* under the control state during the performance of goal-directed reaching task with delay (Figure 1). Neuronal activity in the task was modulated by task events such as, delay period after S1, S2, HR, FI, and RW, and by target direction (Left, Center, Right). Preferred target direction was defined for each neuron as the direction showing the largest amplitude (positive or negative) in each task event.

The representative example of the STN neuron during the task performance is shown in Figure 11. Stimulation of the MI induced biphasic response composed early and late excitation (Figure 11, right bottom corner). Raster plots and spike-density functions (SDFs) of the neuron showed movement-related activity changes. In "Go" trials, there was gradual activity increase after S1 (delay-related activity), phasic activity increase before HR, and another phasic increase before FI. Patterns of movement-related activity were different among Left, Center, and Right target trials: The first increase was large, and the second increase was small in the Right target trials; and the second increase was large and formed two peaks in the Left target trials. In "Stop" trials, this neuron showed different activity patterns among different targets. This neuron showed delay-related activity especially in the Right target trials and activity increase after S2 in the Left target trials, suggesting target dependency of stop related activity. In "NoGo" trials, there is no S1- or S2-related activity changes.

Among 115 STN neurons, in “Go” trials, 76 neurons (66%) were mainly modulated during HR, 29 neurons (26%) showed the strongest response during FI, and four neurons during RW. Almost half of the recorded STN neurons showed modulation of the activity after S1 and in six neurons (5%) among them that response was dominant. These activity changes were activity increase in most STN neurons (86%) in all task events of “Go” trials. Neurons were modulated mostly in Left (41%, n = 47 neurons), Center (27%, 31 neurons), or Right (32%, 37 neurons) target in HR and FI events (actual movement). The high percentage in Left target trials is probably because the monkey needed large movements to reach the left target using its right upper limb. In “Stop” trials, 53 neurons (46%) were modulated mainly during delay period after S1, 36 neurons (32%) changed their activity mainly after S2 presentation, and 24 neurons (21%) demonstrated the highest firing rate changes during RW. These activity changes were activity increase in most STN neurons (90%). They were modulated mostly in Left (38%, n = 44 neurons), Center (19%, 21 neurons), or Right (42%, 48 neurons) target trials in S1 and S2 events. In “NoGo” trials, there were generally no activity changes in relation to the S1 or S2.

Changes of the task-related activity by drugs injections

To explore the contribution of GABAergic and glutamatergic inputs to STN activity during task performance, I injected their antagonists into the STN and observed STN activity in 23 neurons. I tested different order of drugs injections: Gabazine first followed by NBQX and CPP mixture in 22 neurons, and opposite order in one neuron. Three representative examples of STN neurons during task performance are shown in Figure 12 - Figure 18.

The first example of the STN neuron was shown in Figure 12. In the control state in "Go" trials, there was an activity increase before HR and before FI. Amplitudes of the first increase were different among the three targets. In "Stop" and "NoGo" trials, there were no significant changes in the activity in any of task events. After gabazine application into the STN, task-related activity was not changed in Center and Right target trials, and the first peak was increased in Left target trials. In "Stop" trials, the significant peak appeared around 350 ms after S2 in Left target trials. After the additional NBQX and CPP application, sharp peaks of task-related activity in "Go" trials were diminished. In "Stop" trials, the increase after S2 in Left target trials remained. I calculated GABAergic and glutamatergic components by subtracting SDFs before and after drugs injections (Figure 13). This neuron showed significant inhibitory GABAergic and facilitatory glutamatergic components in Left trials of Go trials. Thus, the movement-related response in Figure 12 is formed by biphasic GABAergic inhibitory and glutamatergic facilitatory components (Figure 13). The direction selectivity was observed in both GABAergic and glutamatergic components. There is GABAergic (Left target) and glutamatergic (Right target) inputs in "Stop" trials, and no significant GABAergic and glutamatergic components in "NoGo" trials.

The second example of the STN neuron was shown in Figure 14. Raster and SDFs in control state and after gabazine injection showed two increase in "Go" trials: The first peak around 100-300 ms after S2 and the second peak around 50-130 ms after HR, which were interposed by inhibition during HR. In "Stop" trials, there was also two increase after S2, which were similar to those in Go trials. After additional NBQX and CPP mixture injection, most of responses were lost. In "NoGo" trials, there were no significant responses in control and after gabazine, and NBQX + CPP injection. The analysis of

GABAergic and glutamatergic components revealed that facilitatory GABAergic and facilitatory glutamatergic components in “Go” and “Stop” trials (Figure 15).

The third example was shown in Figure 16. This neuron showed activity increase started 100 ms after HR and ended with FI event in control and after gabazine and NBQX + CPP injection, and activity pattern was similar among three targets. In “Stop” trials, there were no significant changes in the control state, but activity increase after S2 appeared in Left target trials after gabazine. These responses disappeared after additional NBQX+CPP application. This neuron showed no significant changes in “NoGo” trials in control sate and after drug injections. The component analysis revealed that in “Go” trials inhibitory GABAergic and facilitatory glutamatergic components between HR and FI (Figure 17). In Left target trials of “Stop” trials, significant inhibitory GABAergic and facilitatory glutamatergic components were observed within 200 ms after S2 presentation.

Analyses of GABAergic and glutamatergic components

I compared latencies of GABAergic and glutamatergic components after S2 (for details, see *Data Analysis*) (Figure 18). In “Go” trials, GABAergic components (240±117 ms) showed longer latencies than glutamatergic components (162±104 ms) ($p = 0.0178$ paired, one-tailed *t*-test). The similar tendency was observed in “Stop” trials: GABAergic components (163±106 ms) showed longer latencies than glutamatergic components (141±131 ms). In general, the latencies in “Stop” trials were shorter than those in “Go” and “NoGo” trials.

STN neurons can be classified by the polarities of GABAergic and glutamatergic components: I) Inhibitory GABAergic and facilitatory glutamatergic components (n = 9, 39%), II) Facilitatory GABAergic and facilitatory glutamatergic components (n = 8, 35%),

III) Facilitatory GABAergic and inhibitory glutamatergic components (n = 3, 13%), and IV) Inhibitory GABAergic and inhibitory glutamatergic components (n = 3, 13%). Then, I examined the population activity of GABAergic and glutamatergic components of the first group (Figure 19, Figure 20). In "Go" trials, the decrease of GABAergic component was started around 200 ms before HR event and terminated at HR. The second decrease was started after HR and terminated at FI (Figure 19). Glutamatergic component showed a buildup of the activity during delay period and was increased before HR and terminated at HR. The second increase started after HR and reached its peak before FI (Figure 20). There were no significant changes of GABAergic and glutamatergic inputs in "Stop" and "NoGo" trials. I examined DS of GABAergic and glutamatergic components at different task events and found that in "Go" trials at S2 (DS = 0.74 ± 0.26) it was significantly higher ($p = 0.018$ paired, one-tailed *t*-test) than that in "Stop" trials (DS = 0.57 ± 0.36) (Figure 23A). The same tendency was observed at S1 ("Go" trials: DS = 0.69 ± 0.31, "Stop" trials: DS = 0.53 ± 0.41) and no changes in DS at HR, RI, and RW.

I also examined the second group of STN neurons with facilitatory GABAergic and facilitatory glutamatergic component. In "Go" trials, GABAergic component increased after S2, reached its peak around 100-400 ms after S2 and retuned to 0 at HR (Figure 21). It increased after around 150 ms after HR and continued after FI. There were no significant changes in "Stop" and "NoGo" trials. Glutamatergic component showed a similar tendency to that in GABAergic component in "Go" trials (Figure 22). Glutamatergic component also showed buildup activity during delay period after S1 in "Go" and "Stop" trials and increase after S2 in "Stop" trials. Stop-related glutamatergic activity reached its peak at 85 ms after S2, which was shorter than that of movement-related activity in "Go" trials, and retuned to 0 around 100 ms after RW. This long-lasting

increase was observed in “Go”, “Stop” and “NoGo” trials. I examined DS of GABAergic and glutamatergic components at different task events and found no significant changes in DS at different task events of the second group (Figure 23B).

Number of the third and fourth groups was small and not further analyzed.

Among the recorded neurons, GABAergic component (n = 5) and glutamatergic component (n = 7) showed a gradual decrease and gradual increase activity during the delay period, respectively. Inhibitory GABAergic component was small, and only facilitatory glutamatergic component was analyzed. In “Go” and “Stop” trials, the glutamatergic component started to increase around 200 ms after S1 (Figure 24). In “Go” trials, it continued around 150 ms after S2, corresponding to the movement onset. In “Stop” trials, it retuned to the baseline around 500 ms after S2.

EMG activity during task performance

Figure 25 shows a typical example of EMG activity during task performance. EMG was aligned with S2 signal for all types of trials. In “Go” trials, significant activity changes were observed within the actual movement for wrist extensor, wrist flexor, biceps brachii, triceps brachii, trapezius, and deltoid in all target directions. There were no significant changes in muscle activity within the delay period. All muscles, except triceps brachii and deltoid, showed different activity among Left, Center, and Right targets, and this may determine the direction of reaching. In “Stop” and “NoGo” trials, no significant changes in EMG activity were detected.

Discussion

Cortical stimulation induced bi-phasic response composed of early excitation and late excitation intervened by a short gap. In the present study, I examined the responsible pathway for each response component. Our findings suggest that 1) early excitation and late excitation in the STN induced by cortical stimulation are mediated by the *hyperdirect* and *indirect* pathways, respectively, 2) the cortico-STN-GPe-STN transmission has little effects on cortically evoked responses in the STN, and 3) the cortico-STN transmission is mainly mediated by NMDA receptors. These results support the first hypothesis regarding the origin of the cortically evoked biphasic response in the STN: Early and late excitations are mediated by the *hyperdirect* and *indirect* pathways, respectively. These results largely agree with previous studies in rodents (Kitai et al. 1981, Rouzaire-Dubois et al. 1987, Fujimoto et al. 1993, Maurice et al. 1998). However, other rodent study reported the cortico-STN-GPe-STN transmission induced inhibition in the STN.

In the second part of the study, STN neuronal activity during the performance of "Go/Stop/NoGo" goal-directed reaching task with delay was recorded, and their origins were analyzed. The results showed that MI-receiving region in the STN is involved in both motor execution and cancellation. Task-related STN activity was also controlled through *direct* glutamatergic and *indirect* GABAergic inputs from the cortex. The stop-related activity was mainly transmitted through the *hyperdirect* pathway that caused facilitation in the STN, while the role of the *indirect* pathway was minor. The DS was evident in both "Go" and "Stop" trials, suggesting that some neurons with stop-related activity involved in a specific stop, while other neurons participated in a global stop.

Origin of early excitation

The present study demonstrated the decrease of cortically evoked early excitation in the STN after local injection of NBQX and CPP into the STN, suggesting that the early excitation is mediated by ionotropic glutamatergic inputs probably from the cortex. However, the weak response still remained according to population data (Figure 5A3), probably because of the following reasons: (1) Different types of receptors, such as metabotropic glutamate receptors (Kuwajima et al. 2004, Galvan et al. 2006), which are involved in the maintenance of STN spontaneous firing, may also partly contribute to the early excitation, and (2) NBQX and CPP injection could not entirely cover large dendritic fields of STN neurons (Rafols et al. 1976, Afsharpour 1985, Sato et al. 2000), especially distal dendrites, where glutamatergic receptors are expressed abundantly (Smith et al. 1988).

To examine whether this effect was mediated by NMDA or AMPA/kainate receptors, NBQX and CPP were applied separately. NBQX had no effect on the early excitation, whereas additional application of CPP almost diminished the early excitation (Figure 5B). These results suggest the involvement of NMDA receptors, but not AMPA/kainate receptors, in the glutamatergic cortico-STN transmission. Previous anatomical and physiological studies described existence of both NMDA and AMPA/kainate receptors in STN neurons (Clarke et al. 1998, Wang et al. 2000, Smith et al. 2001, Swanger et al. 2015) and fast AMPA and slow long-lasting NMDA-mediated excitatory responses (Mouroux et al. 1993, Gotz et al. 1997, Ozawa et al. 1998, Nambu et al. 2000, Wilson et al. 2004). STN neurons are spontaneously active, and NMDA receptors might be activated and be easily involved in cortico-STN neurotransmission. It was also reported that NMDA receptors play a major role in cortico-STN

neurotransmission of parkinsonian states in rodents (Pan et al. 2014) and nonhuman primates (Bhattacharya et al. 2018). Actually NMDA receptors, not AMPA/kainate receptors, are considered as potential therapeutic targets for PD (Luquin et al. 1993, Blandini et al. 2001, Hallett et al. 2004, Swanger et al. 2015).

Origin of late excitation

Cortically induced late excitation in the STN was not completely, but partly suppressed by gabazine local injection into the STN (Figure 5A, C), suggesting involvement of the GPe-STN GABAergic projections. Blockade of cortico-striato-GPe-STN pathways by muscimol injection into the putamen or striatum significantly decreased late excitation in the STN (Figure 7A, Figure 8A). Gabazine injection into the GPe was expected to suppress cortically induced inhibition in the GPe, which was mediated by cortico-striato-GPe pathway (Kita et al. 2004), also decreased late excitation in the STN (Figure 8B). These results support that cortically induced late excitation in the STN is caused by disinhibition from the GPe through the cortico-striato-GPe *indirect* pathway. The mechanism that gabazine injection into the STN could not totally suppress cortically evoked late excitation in the STN remains to be elucidated. But following explanations could be considered: (1) STN neurons have their intrinsic membrane properties regulating firings (Farries et al. 2010), and blockade of GABAergic inputs could not increase spontaneous firing rates to the level of late excitation, and (2) Other transmissions, such as $GABA_B$ receptors in the STN (Galvan et al. 2004, Charara et al. 2005) may contribute to tonic inhibition and phasic disinhibition by the GPe.

Cortically induced late excitation in the STN tended to be suppressed after local NBQX or NBQX + CPP application into the STN (Figure 5). This is probably because

spontaneous firing rates were decreased after NBQX or NBQX + CPP application, and disinhibition from the GPe could not release enough firing increase. The previous report suggests that glutamatergic local axon collaterals of STN neurons maintain spontaneous activity (Smith et al. 1988, Gouty-Colomer et al. 2018). This amplifying mechanism might also contribute to late excitation.

Origin of gap

The GPe receives cortical inputs through the cortico-STN-GPe pathway, which induces early excitation in the STN evoked by cortical stimulation (Kita 1992, Nambu et al. 2000, Jaeger et al. 2011). I examined the possibility that the early excitation in the GPe may contribute to the gap in the STN thorough the GABAergic inhibitory GPe-STN projections. Local gabazine injection into the STN did not affect the gap (Figure 5C3). NBQX injection into the GPe, which was supposed to suppress early excitation in the GPe (Kita et al. 2004) did not affect the gap (Figure 8C). These results suggest that the gap is not active GABAergic inhibition from the GPe, but a simple absence of excitations.

Origin of long-lasting late inhibition

Cortical stimulation usually induced long-lasting inhibition after biphasic response followed by long-lasting excitation. In the present study, I did not intend to clarify the origin of these responses. These responses were resistance to pharmacological manipulations in the present study, suggesting the origin outside the basal ganglia. Most probable origin is disfacilitation and facilitation from the cortex after the stimulation, which was also observed in the putamen (Nambu et al. 2002).

Spontaneous activity changes

Local application of CPP and NBQX in the vicinity of recorded STN neurons decreased the firing rate. Thus, glutamatergic cortical inputs are the major driving forces to maintain STN neuronal activity. In the case of gabazine injection into the STN, spontaneous firing rates were increased. The spontaneous firing rates were decreased after gabazine injection into the GPe, and were increased after muscimol injection into the GPe. These results suggest that STN activity is also controlled by tonic GABAergic inputs from the GPe. On the other hand, muscimol injection into the putamen had no effect on STN spontaneous firing rates, probably because striatal neurons show low base firing rate (Nambu et al. 2002).

Firing patterns of STN neurons were resistant to drug manipulation except for increased CV after gabazine injection into the STN and increased BI and CV after gabazine injection into the GPe, which is contrast those observed in GPe and GPi (Kita et al. 2004, Kita et al. 2006, Tachibana et al. 2008). This is probably because STN neurons have their intrinsic membrane properties maintaining spontaneous activity (Nakanishi et al. 1987). On the other hand, gabazine injection into the GPe increased spontaneous activity and induced bursts (Kita et al. 2004) probably because of intrinsic cellular properties, pacemaker mechanism of GPe neurons (Plenz et al. 1999, Jaeger et al. 2011), which finally induced burst activity in the STN.

Functional considerations

In the present study, I have clearly shown that the STN receives cortical inputs mainly through the cortico-STN *hyperdirect* and cortico-striato-GPe-STN *indirect* pathways. The contribution of other pathways, such as cortico-STN-GPe-STN pathway,

is less probable. I used electrical stimulation in the motor cortices in the present study, but activity in the cortex is similarly transmitted along the cortico-basal ganglia pathway during voluntary movements, thus electrical stimulation can mimic information flow during movements. STN neurons were reported to increase their activity during upper limb or eye movements during task performance (Delong et al. 1984, Delong et al. 1985, Matsumura et al. 1992, Wichmann et al. 1994). More recent reports emphasized STN activity related changing or canceling tasks or movements (Aron et al. 2006, Isoda et al. 2008, Pasquereau et al. 2017, Schmidt et al. 2017), because STN activity increases GPi activity, decreases thalamo-cortical activity, and finally has suppressive effects on movements. The activity in the STN during task performance is also considered to be mediated by the cortico-STN *hyperdirect* or cortico-striato-GPe-STN *indirect* pathways, and contribution of each pathway to the activity during task performance remains to be elucidated.

The STN activity finally transmitted to the GPi and substantia nigra pars reticulata (SNr), output nuclei of the basal ganglia and contributed control of voluntary movements. The cortical stimulation induced early excitation, inhibition and late excitation in the GPe and GPi/SNr. It is highly probable that early and late excitation in the STN induces early and late excitation in the GPe and GPi/SNr (Nambu et al. 2000, Kita et al. 2004, Tachibana et al. 2008). Based on the cortically evoked responses, I have proposed the dynamic model of the basal ganglia functions: signals through the cortico-STN-GPi/SNr *hyperdirect* pathway reset ongoing cortical activity, signals through the cortico-striato-GPe/SNr *direct* pathway disinhibit thalamo-cortical activity and release appropriate movements, and finally signals through the cortico-striato-GPe-STN-GPi/SNr *indirect* pathway inhibit thalamo-cortical activity and stop movements.

Clinical significance

I sometimes observed dyskinetic movements after gabazine injection into the GPe (Crossman et al. 1984, Grabli et al. 2004). This manipulation suppressed cortically induced late excitation in the STN. Specific ablation of striato-GPe indirect pathway neurons increased locomotor activity in mice (Sano et al. 2003). They did not observe STN activity but found that cortically induced late excitation was lost in the SNr. These observations suggest that cortically induced late excitation play a role to suppress or stop movements. Moreover, STN lesion or blockade induced hemiballism (Whittier et al. 1949, Carpenter et al. 1950, Hamada et al. 1992, Nambu et al. 2000), this may be explained the loss of stop signals from the basal ganglia.

Lesions or chronic high-frequency stimulation (deep brain stimulation, DBS) in the STN ameliorate PD symptoms (Bergman et al. 1990, Aziz et al. 1991, Pollak et al. 1993, Benabid et al. 1994, Limousin et al. 1995). Especially STN-DBS is now important option for advanced PD patients. These procedures affect all components in the STN, such as afferent inputs through the *hyperdirect* and *indirec*t pathways and STN neuronal activity. This is the basic knowledge to understand the therapeutic mechanism of STN-DBS and to develop new DBS therapy.

Role of the hyperdirect and indirect pathways in the STN movement-related activity

I used goal-directed reaching task with delay that includes "Go/Stop/NoGo" trials in order to clarify the role of *hyperdirect* and *indirect* pathways on the STN movement-related activity. *Monkey S* was trained to perform the task for more than 6 months to reach fast reaction time, which is important for revealing preparatory activity after the beginning of the trial. The success rate reached more than 95% in "Go" and "NoGo" trials

and 99% in “Stop” trials. Thus, in the present study, I take into consideration only correct trials.

The analysis of the task-related neuronal activity in the control state revealed its complex activity changes in the large portion of STN neurons. The strong modulation of the activity occurred during actual movement in the majority of recorded units. I detected the presence of direction selectivity in both “Go” and “Stop” trials, which was higher for the Left/Right target trials compare to the Center target trials. The observed pattern of neuronal activity with multiple peaks and target selectivity might be caused by the task complexity (Greenhouse et al. 2015, Fischer et al. 2016) and the influence of the *hyperdirect* and *indirect* pathways.

The majority of neurons were involved in the actual movement in “Go” trials and 32% of them were modulated at S2 in “Stop” trials, which means roles of STN neurons in both processes: motor program execution and cancellation. That observation agreed with studies on monkeys (Pasquereau et al. 2017) and humans (Benis et al. 2016). There were no activity changes in “NoGo” trials, which is similar to putaminal neurons (Takara et al. 2011). The results of my study also showed delay-related activity after S1, suggest the involvement of the STN in motor planning (Thobois et al. 2000, Fischer et al. 2017).

In the present study, stop-related activity was detected in the dorsolateral part of the STN (MI domain) according to the organization of cortico-STN inputs (Nambu et al. 2002). Previous reports showed involvement of the ventral region of the STN in stop action (Isoda et al. 2008, Bastin et al. 2014, Pasquereau et al. 2017) or stop-related activity in the dorsal area of the STN in humans (Benis et al. 2016). The role of MI-receiving

territory of the STN in motor control has not been studied in details using primates or humans.

It was shown that "Go" and "Stop" signals might trigger independent processes that compete between each other (Logan et al. 1984, Verbruggen et al. 2009). In the present study, I revealed that both supportive and competitive inputs from the *hyperdirect* and *indirect* pathways participated in the formation of the STN movement-related activity. The analysis of GABAergic and glutamatergic components revealed that both inputs participated in positive or negative action on STN neurons. The majority of neurons have facilitatory glutamatergic component and either inhibitory or facilitatory GABAergic components. The dominance of facilitatory glutamatergic component might be caused by the cortical high firing rate, which may cause facilitation (increased inputs) or disfacilitation (decreased inputs) in the STN. The GABAergic inputs were transmitted through both active inhibition and disinhibition from the GPe.

I suggest two main types of information transmission through the *hyperdirect* and *indirect* pathways. There are several possibilities. 1) Inputs from the *hyperdirect* and *indirect* pathways compete with each other. 2) Glutamatergic facilitation through the *hyperdirect* pathway is supported by disinhibition from the GABAergic input through the indirect pathway. The stop-related activity is linked to the group of neurons with facilitation that transmitted through glutamatergic inputs and disinhibition that comes through GABAergic inputs (Figure 21, Figure 22). According to the classic BG model, the role of the STN in stopping motor responses is realized by means of the inhibitory *indirect* pathway (Bogacz et al. 2007, Isoda et al. 2008). However, the idea of stop-related

information transmission through the *hyperdirect* pathway was suggested previously based on human fMRI and single-unit recordings (Aron et al. 2016).

It was revealed that the buildup activity after the instruction signal was mainly caused by the glutamatergic component (Figure 24), however, in some neurons it also carried through the GABAergic input. It is known that the STN receives glutamatergic inputs (Chu et al. 2015, Chu et al. 2017), which may contribute to changes in the STN firing rate and, consequently, play the role in the adjustment of movement-related activity. Our results demonstrated that glutamatergic inputs are relevant in both motor planning and cancellation. Thus, it might be involved in the action initiation processes (Benis et al. 2016).

Neurons with contradictive inputs show high DS at instruction and triggering signals in "Go" trials in comparison with "Stop" trials (Figure 23A), which might play a role in global stop (Aron 2011, Benis et al. 2016). The group of neurons with supportive inputs has no significant difference of DS between "Go" and "Stop" trials that might play a role in specific stop (Aron 2011) (Figure 23B).

To confirm that stop-related STN activity is not related to activation of any muscles, such as antagonist muscle, I recorded EMG activity of wrist extensor, wrist flexor, biceps brachii, triceps brachii, trapezius, and deltoid during the task performance (Figure 25). The results demonstrated significant changes within the actual movement in "Go" trials and no activity in "Stop" and "NoGo" trials. Thus, STN neuronal activity in "Stop" trials is not caused by muscles activity.

Conclusions

The present results suggest that the STN receives direct information from the cortex, which is mediated through NMDA receptors, and contributed to the early excitation. The late excitation is originated from cortical information through the *indirect* pathway and GABAergic projections (Figure 26). The biphasic response with a short gap between two excitations is possibly due to unique membrane properties of STN neurons that modulate action potentials quicker than in striatal neurons (Farries et al. 2010). Moreover, the conduction velocities of STN axons are faster than of striatal axons (Tremblay et al. 1989). These features of the STN makes it possible to be involved in the complex regulation of movement-related activity. In the present study, I demonstrated the involvement of both pathways to the motor program execution and cancellation by the STN, which is supported with findings of the existence of different firing patterns: some STN neurons increase while others decrease activity in the movements (Bastin et al. 2014, Zavala et al. 2015). Moreover, I revealed that stop-related activity is transmitted through the *hyperdirect* pathway while the *indirect* pathway shows minor function. Our present data are consistent with the idea that the STN is a key structure of BG and plays important role in the control of voluntary movements and motor learning (Nambu et al. 2002, Hamani et al. 2004, Frank 2006).

The conclusions of the present study are very important to understand not only the normal functions of the STN but also the pathophysiology of STN-related disorders and the therapy targeting at the STN. Lesions or applying high frequency stimulation in the STN ameliorates parkinsonian symptoms. These procedures affect all components in the STN, such as afferent inputs through the *hyperdirect* and *indirec*t pathways and STN neuronal activity. If we can understand which component is most affected by such

procedures, we may find more effective manipulating targets or methods to treat Parkinson's disease.

References

Afsharpour, S. (1985). "Light microscopic analysis of Golgi-impregnated rat subthalamic neurons." J Comp Neurol **236**(1): 1-13.

Alexander, G. E. and M. D. Crutcher (1990). "Functional architecture of basal ganglia circuits: neural substrates of parallel processing." Trends Neurosci **13**(7): 266-271.

Alexander, G. E., M. D. Crutcher and M. R. DeLong (1990). "Basal ganglia-thalamocortical circuits: parallel substrates for motor, oculomotor, "prefrontal" and "limbic" functions." Prog Brain Res **85**: 119-146.

Aron, A. R. (2011). "From reactive to proactive and selective control: developing a richer model for stopping inappropriate responses." Biol Psychiatry **69**(12): e55-68.

Aron, A. R., D. M. Herz, P. Brown, B. U. Forstmann and K. Zaghloul (2016). "Frontosubthalamic Circuits for Control of Action and Cognition." J Neurosci **36**(45): 11489-11495.

Aron, A. R. and R. A. Poldrack (2006). "Cortical and subcortical contributions to Stop signal response inhibition: role of the subthalamic nucleus." J Neurosci **26**(9): 2424-2433.

Aziz, T. Z., D. Peggs, M. A. Sambrook and A. R. Crossman (1991). "Lesion of the subthalamic nucleus for the alleviation of 1-methyl-4-phenyl-1,2,3,6-tetrahydropyridine (MPTP)-induced parkinsonism in the primate." Mov Disord **6**(4): 288-292.

Bastin, J., M. Polosan, D. Benis, L. Goetz, M. Bhattacharjee, B. Piallat, A. Krainik, T. Bougerol, S. Chabardes and O. David (2014). "Inhibitory control and error monitoring by human subthalamic neurons." Transl Psychiatry **4**: e439.

Benabid, A. L., P. Pollak, C. Gross, D. Hoffmann, A. Benazzouz, D. M. Gao, A. Laurent, M. Gentil and J. Perret (1994). "Acute and long-term effects of subthalamic nucleus stimulation in Parkinson's disease." Stereotact Funct Neurosurg **62**(1-4): 76-84.

Benis, D., O. David, B. Piallat, A. Kibleur, L. Goetz, M. Bhattacharjee, V. Fraix, E. Seigneuret, P. Krack, S. Chabardes and J. Bastin (2016). "Response inhibition rapidly increases single-neuron responses in the subthalamic nucleus of patients with Parkinson's disease." Cortex **84**: 111-123.

Bergman, H., T. Wichmann and M. R. DeLong (1990). "Reversal of experimental parkinsonism by lesions of the subthalamic nucleus." Science **249**(4975): 1436-1438.

Bergman, H., T. Wichmann, B. Karmon and M. R. DeLong (1994). "The primate subthalamic nucleus. II. Neuronal activity in the MPTP model of parkinsonism." J Neurophysiol **72**(2): 507-520.

Bhattacharya, S., Y. Ma, A. R. Dunn, J. M. Bradner, A. Scimemi, G. W. Miller, S. F. Traynelis and T. Wichmann (2018). "NMDA receptor blockade ameliorates abnormalities of spike firing of subthalamic nucleus neurons in a parkinsonian nonhuman primate." J Neurosci Res **96**(7): 1324-1335.

Blandini, F., G. Nappi and J. T. Greenamyre (2001). "Subthalamic infusion of an NMDA antagonist prevents basal ganglia metabolic changes and nigral degeneration in a rodent model of Parkinson's disease." Ann Neurol **49**(4): 525-529.

Bogacz, R. and K. Gurney (2007). "The basal ganglia and cortex implement optimal decision making between alternative actions." Neural Comput **19**(2): 442-477.

Carpenter, M. B., J. R. Whittier and F. A. Mettler (1950). "Analysis of choreoid hyperkinesia in the Rhesus monkey; surgical and pharmacological analysis of hyperkinesia resulting from lesions in the subthalamic nucleus of Luys." J Comp Neurol **92**(3): 293-331.

Charara, A., J. F. Pare, A. I. Levey and Y. Smith (2005). "Synaptic and extrasynaptic GABA-A and GABA-B receptors in the globus pallidus: an electron microscopic immunogold analysis in monkeys." Neuroscience **131**(4): 917-933.

Chu, H. Y., J. F. Atherton, D. Wokosin, D. J. Surmeier and M. D. Bevan (2015). "Heterosynaptic regulation of external globus pallidus inputs to the subthalamic nucleus by the motor cortex." Neuron **85**(2): 364-376.

Chu, H. Y., E. L. McIver, R. F. Kovaleski, J. F. Atherton and M. D. Bevan (2017). "Loss of Hyperdirect Pathway Cortico-Subthalamic Inputs Following Degeneration of Midbrain Dopamine Neurons." Neuron **95**(6): 1306-1318 e1305.

Clarke, N. P. and J. P. Bolam (1998). "Distribution of glutamate receptor subunits at neurochemically characterized synapses in the entopeduncular nucleus and subthalamic nucleus of the rat." J Comp Neurol **397**(3): 403-420.

Crossman, A. R., M. A. Sambrook and A. Jackson (1984). "Experimental hemichorea/hemiballismus in the monkey. Studies on the intracerebral site of action in a drug-induced dyskinesia." Brain **107 (Pt 2)**: 579-596.

DeLong, M. R. (1990). "Primate models of movement disorders of basal ganglia origin." Trends Neurosci **13**(7): 281-285.

Delong, M. R., M. D. Crutcher and A. P. Georgopoulos (1985). "Primate Globus Pallidus and Subthalamic Nucleus - Functional-Organization." Journal of Neurophysiology **53**(2): 530-543.

Delong, M. R., A. P. Georgopoulos, M. D. Crutcher, S. J. Mitchell, R. T. Richardson and G. E. Alexander (1984). "Functional organization of the basal ganglia: contributions of single-cell recording studies." Ciba Found Symp **107**: 64-82.

Farries, M. A., H. Kita and C. J. Wilson (2010). "Dynamic spike threshold and zero membrane slope conductance shape the response of subthalamic neurons to cortical input." J Neurosci **30**(39): 13180-13191.

Fife, K. H., N. A. Gutierrez-Reed, V. Zell, J. Bailly, C. M. Lewis, A. R. Aron and T. S. Hnasko (2017). "Causal role for the subthalamic nucleus in interrupting behavior." Elife **6**.

Fischer, P., A. Pogosyan, B. Cheeran, A. L. Green, T. Z. Aziz, J. Hyam, S. Little, T. Foltynie, P. Limousin, L. Zrinzo, M. Hariz, M. Samuel, K. Ashkan, P. Brown and H. Tan (2017). "Subthalamic nucleus beta and gamma activity is modulated depending on the level of imagined grip force." Exp Neurol **293**: 53-61.

Fischer, P., H. Tan, A. Pogosyan and P. Brown (2016). "High post-movement parietal low-beta power during rhythmic tapping facilitates performance in a stop task." Eur J Neurosci **44**(5): 2202-2213.

Frank, M. J. (2006). "Hold your horses: a dynamic computational role for the subthalamic nucleus in decision making." Neural Netw **19**(8): 1120-1136.

Fujimoto, K. and H. Kita (1993). "Response characteristics of subthalamic neurons to the stimulation of the sensorimotor cortex in the rat." Brain Res **609**(1-2): 185-192.

Galvan, A., A. Charara, J. F. Pare, A. I. Levey and Y. Smith (2004). "Differential subcellular and subsynaptic distribution of GABA(A) and GABA(B) receptors in the monkey subthalamic nucleus." Neuroscience **127**(3): 709-721.

Galvan, A., M. Kuwajima and Y. Smith (2006). "Glutamate and GABA receptors and transporters in the basal ganglia: what does their subsynaptic localization reveal about their function?" Neuroscience **143**(2): 351-375.

Galvan, A. and T. Wichmann (2008). "Pathophysiology of parkinsonism." Clin Neurophysiol **119**(7): 1459-1474.

Gotz, T., U. Kraushaar, J. Geiger, J. Lubke, T. Berger and P. Jonas (1997). "Functional properties of AMPA and NMDA receptors expressed in identified types of basal ganglia neurons." J Neurosci **17**(1): 204-215.

Gouty-Colomer, L. A., F. J. Michel, A. Baude, C. Lopez-Pauchet, A. Dufour, R. Cossart and C. Hammond (2018). "Mouse subthalamic nucleus neurons with local axon collaterals." J Comp Neurol **526**(2): 275-284.

Grabli, D., K. McCairn, E. C. Hirsch, Y. Agid, J. Feger, C. Francois and L. Tremblay (2004). "Behavioural disorders induced by external globus pallidus dysfunction in primates: I. Behavioural study." Brain **127**(Pt 9): 2039-2054.

Greenhouse, I., D. Saks, T. Hoang and R. B. Ivry (2015). "Inhibition during response preparation is sensitive to response complexity." J Neurophysiol **113**(7): 2792-2800.

Hallett, P. J. and D. G. Standaert (2004). "Rationale for and use of NMDA receptor antagonists in Parkinson's disease." Pharmacol Ther **102**(2): 155-174.

Hamada, I. and M. R. Delong (1992). "Excitotoxic Acid Lesions of the Primate Subthalamic Nucleus Result in Transient Dyskinesias of the Contralateral Limbs." Journal of Neurophysiology **68**(5): 1850-1858.

Hamani, C., J. A. Saint-Cyr, J. Fraser, M. Kaplitt and A. M. Lozano (2004). "The subthalamic nucleus in the context of movement disorders." Brain **127**(Pt 1): 4-20.

Hanson, T. L., A. M. Fuller, M. A. Lebedev, D. A. Turner and M. A. Nicolelis (2012). "Subcortical neuronal ensembles: an analysis of motor task association, tremor, oscillations, and synchrony in human patients." J Neurosci **32**(25): 8620-8632.

Hassani, O. K., M. Mouroux and J. Feger (1996). "Increased subthalamic neuronal activity after nigral dopaminergic lesion independent of disinhibition via the globus pallidus." Neuroscience **72**(1): 105-115.

Hikosaka, O., Y. Takikawa and R. Kawagoe (2000). "Role of the basal ganglia in the control of purposive saccadic eye movements." Physiol Rev **80**(3): 953-978.

Isoda, M. and O. Hikosaka (2008). "Role for subthalamic nucleus neurons in switching from automatic to controlled eye movement." J Neurosci **28**(28): 7209-7218.

Iwamuro, H., Y. Tachibana, Y. Ugawa, N. Saito and A. Nambu (2017). "Information processing from the motor cortices to the subthalamic nucleus and globus pallidus and their somatotopic organizations revealed electrophysiologically in monkeys." Eur J Neurosci **46**(11): 2684-2701.

Jaeger, D. and H. Kita (2011). "Functional connectivity and integrative properties of globus pallidus neurons." Neuroscience **198**: 44-53.

Kita, H. (1992). "Responses of globus pallidus neurons to cortical stimulation: intracellular study in the rat." Brain Res **589**(1): 84-90.

Kita, H., S. Chiken, Y. Tachibana and A. Nambu (2006). "Origins of GABA(A) and GABA(B) receptor-mediated responses of globus pallidus induced after stimulation of the putamen in the monkey." J Neurosci **26**(24): 6554-6562.

Kita, H., A. Nambu, K. Kaneda, Y. Tachibana and M. Takada (2004). "Role of ionotropic glutamatergic and GABAergic inputs on the firing activity of neurons in the external pallidum in awake monkeys." J Neurophysiol **92**(5): 3069-3084.

Kitai, S. T. and J. M. Deniau (1981). "Cortical inputs to the subthalamus: intracellular analysis." Brain Res **214**(2): 411-415.

Kuwajima, M., R. A. Hall, A. Aiba and Y. Smith (2004). "Subcellular and subsynaptic localization of group I metabotropic glutamate receptors in the monkey subthalamic nucleus." J Comp Neurol **474**(4): 589-602.

Li, C. S., P. Yan, R. Sinha and T. W. Lee (2008). "Subcortical processes of motor response inhibition during a stop signal task." Neuroimage **41**(4): 1352-1363.

Limousin, P., P. Pollak, A. Benazzouz, D. Hoffmann, J. F. Le Bas, E. Broussolle, J. E. Perret and A. L. Benabid (1995). "Effect of parkinsonian signs and symptoms of bilateral subthalamic nucleus stimulation." Lancet **345**(8942): 91-95.

Logan, G. D., W. B. Cowan and K. A. Davis (1984). "On the ability to inhibit simple and choice reaction time responses: a model and a method." J Exp Psychol Hum Percept Perform **10**(2): 276-291.

Luquin, M. R., J. A. Obeso, J. Laguna, J. Guillen and J. M. Martinez-Lage (1993). "The AMPA receptor antagonist NBQX does not alter the motor response induced by selective dopamine agonists in MPTP-treated monkeys." Eur J Pharmacol **235**(2-3): 297-300.

Matsumura, M., J. Kojima, T. W. Gardiner and O. Hikosaka (1992). "Visual and oculomotor functions of monkey subthalamic nucleus." J Neurophysiol **67**(6): 1615-1632.

Maurice, N., J. M. Deniau, J. Glowinski and A. M. Thierry (1998). "Relationships between the prefrontal cortex and the basal ganglia in the rat: Physiology of the corticosubthalamic circuits." Journal of Neuroscience **18**(22): 9539-9546.

Mink, J. W. (1996). "The basal ganglia: focused selection and inhibition of competing motor programs." Prog Neurobiol **50**(4): 381-425.

Monakow, K. H., K. Akert and H. Kunzle (1978). "Projections of the precentral motor cortex and other cortical areas of the frontal lobe to the subthalamic nucleus in the monkey." Exp Brain Res **33**(3-4): 395-403.

Mouroux, M. and J. Feger (1993). "Evidence that the parafascicular projection to the subthalamic nucleus is glutamatergic." Neuroreport **4**(6): 613-615.

Nakanishi, H., H. Kita and S. T. Kitai (1987). "Electrical membrane properties of rat subthalamic neurons in an in vitro slice preparation." Brain Res **437**(1): 35-44.

Nambu, A. (2004). "A new dynamic model of the cortico-basal ganglia loop." Prog Brain Res **143**: 461-466.

Nambu, A., M. Takada, M. Inase and H. Tokuno (1996). "Dual somatotopical representations in the primate subthalamic nucleus: evidence for ordered but reversed body-map transformations from the primary motor cortex and the supplementary motor area." J Neurosci **16**(8): 2671-2683.

Nambu, A., H. Tokuno, I. Hamada, H. Kita, M. Imanishi, T. Akazawa, Y. Ikeuchi and N. Hasegawa (2000). "Excitatory cortical inputs to pallidal neurons via the subthalamic nucleus in the monkey." J Neurophysiol **84**(1): 289-300.

Nambu, A., H. Tokuno and M. Takada (2002). "Functional significance of the cortico-subthalamo-pallidal 'hyperdirect' pathway." Neuroscience Research **43**(2): 111-117.

Ozawa, S., H. Kamiya and K. Tsuzuki (1998). "Glutamate receptors in the mammalian central nervous system." Prog Neurobiol **54**(5): 581-618.

Pan, M. K., C. H. Tai, W. C. Liu, J. C. Pei, W. S. Lai and C. C. Kuo (2014). "Deranged NMDAergic cortico-subthalamic transmission underlies parkinsonian motor deficits." J Clin Invest **124**(10): 4629-4641.

Pasquereau, B. and R. S. Turner (2017). "A selective role for ventromedial subthalamic nucleus in inhibitory control." Elife **6**.

Plenz, D. and S. T. Kital (1999). "A basal ganglia pacemaker formed by the subthalamic nucleus and external globus pallidus." Nature **400**(6745): 677-682.

Pollak, P., A. L. Benabid, C. Gross, D. M. Gao, A. Laurent, A. Benazzouz, D. Hoffmann, M. Gentil and J. Perret (1993). "[Effects of the stimulation of the subthalamic nucleus in Parkinson disease]." Rev Neurol (Paris) **149**(3): 175-176.

Rafols, J. A. and C. A. Fox (1976). "The neurons in the primate subthalamic nucleus: a Golgi and electron microscopic study." J Comp Neurol **168**(1): 75-111.

Ray, N. J., J. S. Brittain, P. Holland, R. A. Joundi, J. F. Stein, T. Z. Aziz and N. Jenkinson (2012). "The role of the subthalamic nucleus in response inhibition: evidence from local field potential recordings in the human subthalamic nucleus." Neuroimage **60**(1): 271-278.

Rodriguez-Oroz, M. C., M. Rodriguez, J. Guridi, K. Mewes, V. Chockkman, J. Vitek, M. R. DeLong and J. A. Obeso (2001). "The subthalamic nucleus in Parkinson's disease: somatotopic organization and physiological characteristics." Brain **124**(Pt 9): 1777-1790.

Rouzaire-Dubois, B. and E. Scarnati (1987). "Pharmacological study of the cortical-induced excitation of subthalamic nucleus neurons in the rat: evidence for amino acids as putative neurotransmitters." Neuroscience **21**(2): 429-440.

Sano, H., Y. Yasoshima, N. Matsushita, T. Kaneko, K. Kohno, I. Pastan and K. Kobayashi (2003). "Conditional ablation of striatal neuronal types containing dopamine D2 receptor disturbs coordination of basal ganglia function." J Neurosci **23**(27): 9078-9088.

Sato, F., M. Parent, M. Levesque and A. Parent (2000). "Axonal branching pattern of neurons of the subthalamic nucleus in primates." J Comp Neurol **424**(1): 142-152.

Schall, J. D. and D. C. Godlove (2012). "Current advances and pressing problems in studies of stopping." Curr Opin Neurobiol **22**(6): 1012-1021.

Schmidt, R. and J. D. Berke (2017). "A Pause-then-Cancel model of stopping: evidence from basal ganglia neurophysiology." Philos Trans R Soc Lond B Biol Sci **372**(1718).

Schmidt, R., D. K. Leventhal, N. Mallet, F. J. Chen and J. D. Berke (2013). "Canceling actions involves a race between basal ganglia pathways." Nature Neuroscience **16**(8): 1118-U1194.

Sharp, D. J., V. Bonnelle, X. De Boissezon, C. F. Beckmann, S. G. James, M. C. Patel and M. A. Mehta (2010). "Distinct frontal systems for response inhibition, attentional capture, and error processing." Proc Natl Acad Sci U S A **107**(13): 6106-6111.

Smith, Y., A. Charara, M. Paquet, J. Z. Kieval, J. F. Pare, J. E. Hanson, G. W. Hubert, M. Kuwajima and A. I. Levey (2001). "Ionotropic and metabotropic GABA and glutamate receptors in primate basal ganglia." J Chem Neuroanat **22**(1-2): 13-42.

Smith, Y. and A. Parent (1988). "Neurons of the subthalamic nucleus in primates display glutamate but not GABA immunoreactivity." Brain Res **453**(1-2): 353-356.

Swanger, S. A., K. M. Vance, J. F. Pare, F. Sotty, K. Fog, Y. Smith and S. F. Traynelis (2015). "NMDA Receptors Containing the GluN2D Subunit Control Neuronal Function in the Subthalamic Nucleus." J Neurosci **35**(48): 15971-15983.

Tachibana, Y., H. Kita, S. Chiken, M. Takada and A. Nambu (2008). "Motor cortical control of internal pallidal activity through glutamatergic and GABAergic inputs in awake monkeys." Eur J Neurosci **27**(1): 238-253.

Takara, S., N. Hatanaka, M. Takada and A. Nambu (2011). "Differential activity patterns of putaminal neurons with inputs from the primary motor cortex and supplementary motor area in behaving monkeys." J Neurophysiol **106**(3): 1203-1217.

Thobois, S., P. F. Dominey, J. Decety, P. P. Pollak, M. C. Gregoire, P. D. Le Bars and E. Broussolle (2000). "Motor imagery in normal subjects and in asymmetrical Parkinson's disease: a PET study." Neurology **55**(7): 996-1002.

Tremblay, L. and M. Filion (1989). "Responses of pallidal neurons to striatal stimulation in intact waking monkeys." Brain Res **498**(1): 1-16.

Verbruggen, F. and G. D. Logan (2008). "Automatic and controlled response inhibition: associative learning in the go/no-go and stop-signal paradigms." J Exp Psychol Gen **137**(4): 649-672.

Verbruggen, F. and G. D. Logan (2009). "Models of response inhibition in the stop-signal and stop-change paradigms." Neurosci Biobehav Rev **33**(5): 647-661.

Wang, X. S., W. Y. Ong, H. K. Lee and R. L. Huganir (2000). "A light and electron microscopic study of glutamate receptors in the monkey subthalamic nucleus." J Neurocytol **29**(10): 743-754.

Whittier, J. R. and F. A. Mettler (1949). "Studies on the subthalamus of the rhesus monkey; hyperkinesia and other physiologic effects of subthalamic lesions; with special reference to the subthalamic nucleus of Luys." J Comp Neurol **90**(3): 319-372.

Wichmann, T., H. Bergman and M. R. DeLong (1994). "The primate subthalamic nucleus. I. Functional properties in intact animals." J Neurophysiol **72**(2): 494-506.

Wilson, C. L., M. Puntis and M. G. Lacey (2004). "Overwhelmingly asynchronous firing of rat subthalamic nucleus neurones in brain slices provides little evidence for intrinsic interconnectivity." Neuroscience **123**(1): 187-200.

Zavala, B., S. Damera, J. W. Dong, C. Lungu, P. Brown and K. A. Zaghloul (2017). "Human Subthalamic Nucleus Theta and Beta Oscillations Entrain Neuronal Firing During Sensorimotor Conflict." Cereb Cortex **27**(1): 496-508.

Zavala, B., K. Zaghloul and P. Brown (2015). "The subthalamic nucleus, oscillations, and conflict." Mov Disord **30**(3): 328-338.

Tables & Figures

Table 1. Number of STN neurons tested.

Monkey	K8	K9	Total
Drug injection into STN (33 neurons)			
NBQX+CPP	6	4	10
NBQX	-	2	2
NBQX, then CPP	1	5	6
CPP, then NBQX	1	-	1
NBQX+CPP, then gabazine	1	4	5
Gabazine	2	3	5
Gabazine, then NBQX+CPP	4	-	4
Drug injection into putamen (15 neurons)			
Muscimol	9	3	12
NBQX	-	3	3
Drug injection into GPe (22 neurons)			
Muscimol	3	5	8
NBQX	2	3	5
Gabazine	5	4	9
Total	34	36	70

Number of neurons in the subthalamic (STN) tested with injection of drugs, such as 1, 2, 3, 4-tetrahydro-6-nitro-2, 3-dioxo-benzo[f]quinoxaline-7-sulfonamide disodium (NBQX, AMPA/kainate receptor antagonist), ±3-(2-carboxypiperazin-4-yl)propyl-1-phosphonic

acid (CPP, NMDA receptor antagonist), gabazine ($GABA_A$ receptor antagonist), or muscimol ($GABA_A$ receptor agonist) into the vicinity of recorded STN, putamen or external segment of globus pallidus (GPe) in two monkeys.

Table 2. Latencies, durations, and amplitude of STN responses evoked by MI- and SMA-stimulation.

Cortical stimulating site	Latency (ms ± SD)			Duration (ms ± SD)			Amplitude (spikes ± SD)	
	Early excitation	Gap	Late excitation	Early excitation	Gap	Late excitation	Early excitation	Late excitation
MI (n = 47)	5.4 ± 1.4**	13.4 ± 2.8	16.8 ± 4.1*	8.0 ± 4.2	3.3 ± 2.8**	22.9 ± 11.1	84.0 ± 63.1*	241.9 ± 199.6
SMA (n = 23)	8.1 ± 1.8**	14.2 ± 5.4	20.6 ± 4.9*	6.8 ± 2.3	7.0 ± 5.6**	19.6 ± 7.3	44.8 ± 28.6*	178.3 ± 89.3

Figures indicate latencies in ms (mean ± SD) of each response component (early excitation, gap, and late excitation) in the STN evoked by the stimulation of the forearm regions of the primary motor cortex (MI) and the supplementary motor area (SMA). * $p < 0.01$, ** $p < 0.001$, significantly different each other, Bonferroni test.

Table 3. The effect of local drugs injections on cortically evoked responses of STN neurons.

	Drugs injections into the STN			Drugs injections into the STN			Drugs injections into the STN		
	Control	NBQX + CPP	Gabazine	Control	NBQX	CPP	Control	Gabazine	NBQX+CPP
Early excitation	(n = 15)	(n = 15)	(n = 5)	(n = 8)	(n = 8)	(n = 6)	(n = 9)	(n = 9)	(n = 4)
Amplitude (spikes ± SD)	86.8 ± 82.2	50.0 ± 63.2**	10.6 ± 23.8	41.2 ± 24.2	38.8 ± 26.8	16.6 ± 13.0**	80.7 ± 23.9	69.1 ± 27.9	37.5 ± 15.7
Duration (ms ± SD)	9.1 ± 4.9	6.7 ± 6.1*	1.0 ± 2.2 2.0	6.6 ± 2.4	6.1 ± 3.9	4.8 ± 2.9	10.0 ± 5.2	9.1 ± 4.8	8.0 ± 3.4
Late excitation	(n = 15)	(n = 15)	(n = 5)	(n = 8)	(n = 8)	(n = 6)	(n = 9)	(n = 9)	(n = 4)
Amplitude (spikes ± SD)	261.1 ± 123.6	161.9 ± 168.7*	61.3 ± 131.4*	153.7 ± 82.8	123.7 ± 59.1*	162.5 ± 118.6	150.2 ± 63.4	154.9 ± 143.2	25.2 ± 7.4
Duration (ms ± SD)	26.9 ± 11.4	21.8 ± 17.6	5.0 ± 9.1	20.9 ± 9.5	21.6 ± 10.4	24.0 ± 12.3	21.6 ± 8.3	19.9 ± 9.6	7.00± 2.2
Gap	(n = 15)	(n = 13)	(n = 5)	(n = 8)	(n = 7)	(n = 6)	(n = 9)	(n = 9)	(n = 4)
Duration (ms ± SD)	2.5 ± 2.1	4.6 ± 2.9*	3.0 ± 1.3	5.3 ± 3.3	6.0 ± 2.4	6.0 ± 1.8	2.0 ± 2.3	4.0 ± 4.7	6.5 ± 7.0

Figures indicate amplitudes (spikes ± SD) and durations (ms ± SD) of early excitation, late excitation, and gap. Different drugs were applied in different orders to the vicinity of recorded STN neurons. * $p < 0.05$, ** $p < 0.01$, significantly different between two adjacent columns, one-tailed paired *t*-test.

Table 4. The effect of local drugs injections on spontaneous activity of STN neurons.

	Drugs injections into the STN			Drugs injections into the STN			Drugs injections into the STN		
	Control	NBQX + CPP	Gabazine	Control	NBQX	CPP	Control	Gabazine	NBQX+CPP
	(n = 15)	(n = 15)	(n = 5)	(n = 8)	(n = 8)	(n = 6)	(n = 9)	(n = 9)	(n = 4)
Firing rate (FR) (Hz)	38.8 ± 11.4	32.6 ± 9.7*	43.0 ± 15.3	27.7 ± 17.5	23.7 ± 10.1	21.9 ± 19.3	37.4 ± 21.0	47.3 ± 31.2*	34.4 ± 29.7
Burst index (BI)	2.50 ± 2.13	4.23 ± 5.40	6.64 ± 6.53	2.22 ± 0.51	2.52 ± 0.82	3.76 ± 2.31	1.62 ± 0.73	1.74 ± 0.87	4.64 ± 1.86
Coefficient of variation (CV)	1.10 ± 0.64	1.58 ± 1.04	1.9 ± 1.58**	1.33 ± 0.94	1.18 ± 0.64	1.28 ± 0.57	1.29 ± 1.37	1.08 ± 1.08	1.43 ± 0.53

Figures indicate mean ± SD of firing rates (FR), burst index (BI), and coefficient of variation (CV). Different drugs were applied in different orders to the vicinity of recorded STN neurons. * $p < 0.05$, ** $p < 0.01$, significantly different between two adjacent columns, one-tailed paired *t*-test.

Table 5. The effects of drug injections into the putamen on cortically evoked responses and spontaneous activity in STN neurons.

	Control	Muscimol into putamen
Cortically evoked responses		
Early excitation	(n = 12)	(n = 12)
Amplitude (spikes ± SD)	52.1 ± 41.2	44.5 ± 34.9
Duration (ms ± SD)	6.3 ± 2.8	6.0 ± 3.6
Late excitation	(n = 12)	(n = 12)
Amplitude (spikes ± SD)	188.6 ± 167.3	49.9 ± 43.3*
Duration (ms ± SD)	18.7 ± 6.9	9.3 ± 6.0**
Gap	(n = 12)	(n = 10)
Duration (ms ± SD)	5.9 ± 5.1	6.6 ± 4.4
Spontaneous activity	(n = 12)	(n = 12)
Firing rate (FR) (Hz)	30.1 ± 16.7	24.3 ± 15.2
Burst index (BI)	3.0 ± 1.0	2.9 ± 1.9
Coefficient of variation (CV)	1.2 ± 0.4	1.1 ± 0.5

* $p < 0.05$, ** $p < 0.01$ significantly different from control, one-tailed paired *t*-test.

Table 6. The effects of drug injections into the GPe on cortically evoked responses and spontaneous activity in STN neurons.

	Drugs injections into the GPe		Drugs injections into the GPe		Drugs injections into the GPe	
	Control	Gabazine	Control	Muscimol	Control	NBQX
Cortically evoked responses						
Early excitation	(n = 9)	(n = 9)	(n = 8)	(n = 8)	(n = 5)	(n = 5)
Amplitude (spikes ± SD)	63.4 ± 58.5	51.4 ± 50.1	74.7 ± 64.7	46.5 ± 49.2	85.5 ± 70.9	85.0 ± 43.4
Duration (ms ± SD)	6.3 ± 2.1	6.6 ± 1.7	6.8 ± 2.6	5.4 ± 2.2	7.0 ± 3.2	9.0 ± 1.2
Late excitation	(n = 9)	(n = 9)	(n = 8)	(n = 8)	(n = 5)	(n = 5)
Amplitude (spikes ± SD)	163.7 ± 86.4	28.4 ± 26.0**	248.8 ± 190.0	73.4 ± 88.6*	355.8 ± 332.5	202.3 ± 113.9
Duration (ms ± SD)	15.6 ± 7.0	10.4 ± 10.5**	21.1 ± 12.3	9.6 ± 6.4*	22.4 ± 11.4	19.6 ± 6.4
Gap	(n = 9)	(n = 6)	(n =8)	(n = 7)	(n = 5)	(n = 5)
Duration (ms ± SD)	6.0 ± 3.0	9.2 ± 3.8*	6.5 ± 3.7	7.4 ± 3.7	6.8 ± 9.7	4.8 ± 7.1
Spontaneous activity	(n = 9)	(n = 9)	(n = 8)	(n = 8)	(n = 5)	n = 5
Firing rate (FR) (Hz)	31.1 ± 20.4	11.5 ± 10.2**	48.6 ± 23.2	61.6 ± 23.9*	33.1 ± 16.0	44.9 ± 25.5
Burst index (BI)	3.1 ± 1.7	14.0 ± 12.5*	1.8 ± 0.5	1.9 ± 0.3	3.0 ± 0.7	4.0 ± 1.5
Coefficient of variation (CV)	1.1 ± 0.4	1.6 ± 0.6*	0.8 ± 0.2	0.9 ± 0.3	1.4 ± 0.3	1.5 ± 0.5

* $p < 0.05$, ** $p < 0.01$ significantly different from control, one-tailed paired *t*-test.

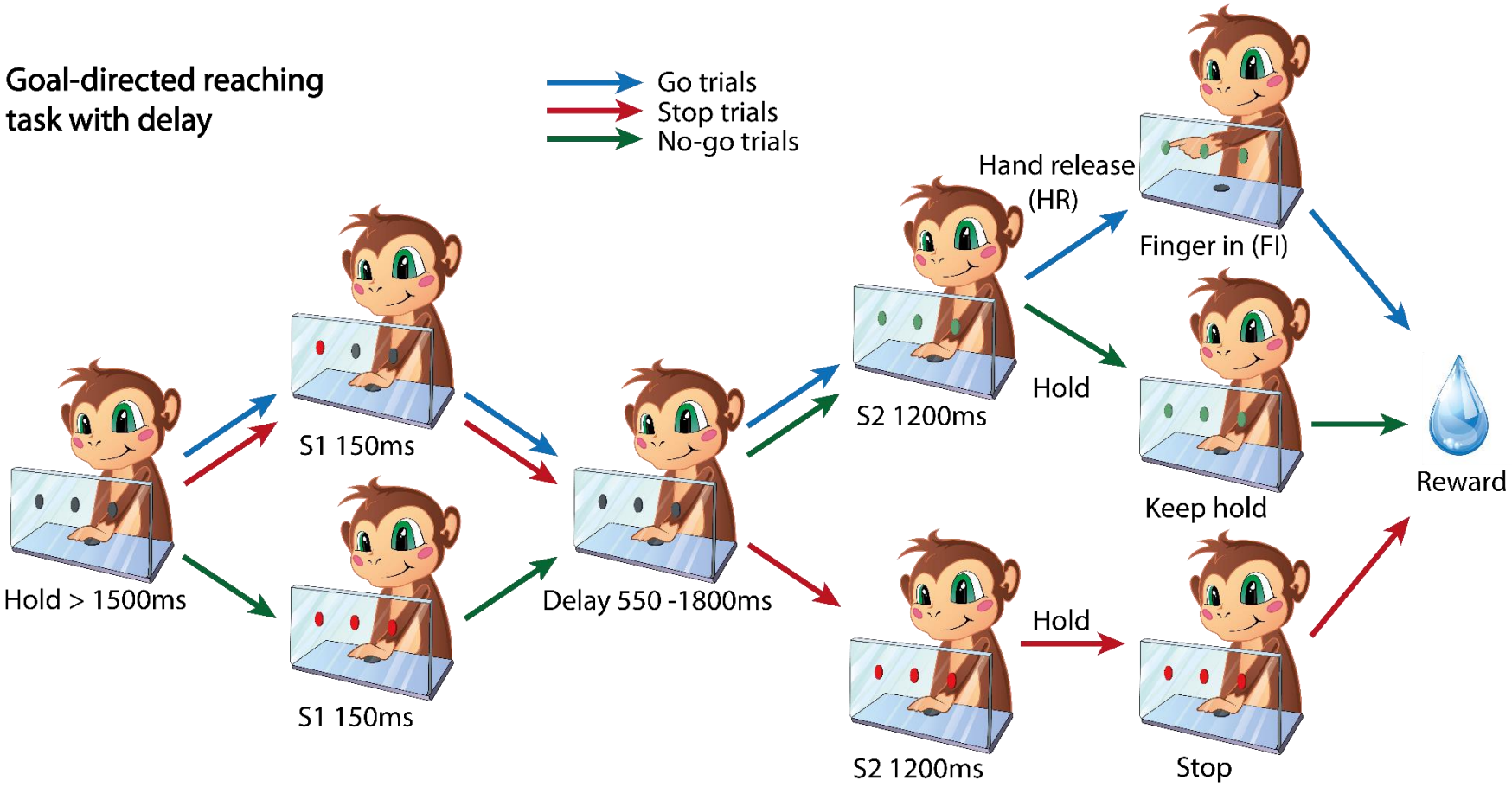
Goal-directed reaching task with delay
Go trials
Stop trials
No-go trials
Hold > 1500ms
S1 150ms
S1 150ms
Delay 550 -1800ms
S2 1200ms
Hand release (HR)
Finger in (FI)
Hold
Keep hold
Reward
Hold
S2 1200ms
Stop

Figure 1

Figure 1. Goal-directed reaching task with delay.

A touch panel with three light-emitting diodes (LEDs) with two colors (green and red) and resting position were set in the front of the monkey. Each trial was initiated after the animal placed its hand at the resting position that was located below the touch panel for at least 1,500 ms. After the task initiation, there were three options of trials. “Go” trials (blue arrow): one of three LEDs was lit with red color as an instruction signal (S1). It was followed by a random delay period. During the instruction signal and delay period, the monkey was required to keep its hand at the resting position. After a delay period, all three LEDs were lit with green color as a triggering signal (S2). During that time, the monkey was required to reach the LED inside the slot that had been presented previously as the instruction signal (S1). If the monkey touched the correct LED within 1,200 ms, it was rewarded with sweetened water. In the case of mistake, the trial with the same task conditions was repeated. The timing of hand release (HR) from the resting position and finger in (FI) to the slot was detected. “Stop” trials (red arrow): the task initiation and first stages before delay period were the same with “Go” trials. All three LEDs were lit with red color (S2). If the monkey kept its hand at the resting position during the entire delay and triggering-signal periods, it was rewarded. “NoGo” trials (green arrow): after task initiation all three LEDs were lit simultaneously with red color as an instruction signal (S1). After a delay period all three LEDs were lit with green color (S2). In that case, the monkey was required to keep its hand at the resting position during the entire delay and triggering- signal periods to get the reward.

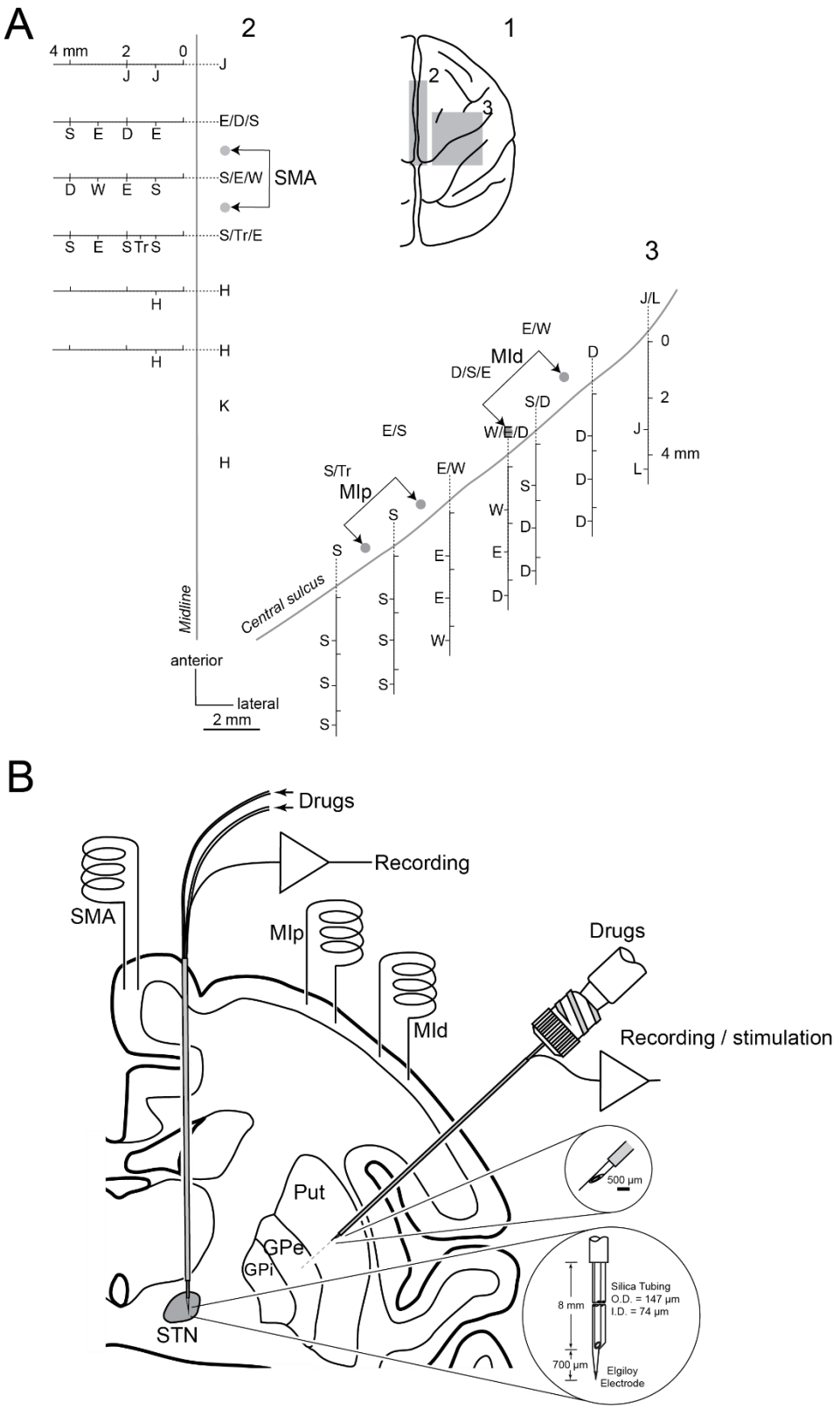
A
2
1
3
4 mm
2
0
J
J J
E/D/S
S E D E
S/E/W
SMA
D W E S
S/Tr/E
S E STr S
H
K
Midline
anterior
lateral
2 mm
Central sulcus
J/L
E/W
MId
D/S/E
S/D
E/S
W/E/D
S/Tr
MIp
B
Drugs
Recording
SMA
MIp
MId
Drugs
Recording / stimulation
Put
GPe
GPi
STN
500 µm
Silica Tubing
O.D. = 147 µm
I.D. = 74 µm
8 mm
700 µm
Elgiloy
Electrode

Figure 2

Figure 2. Cortical mapping and schematic representation of the experimental setup.

A) Cortical mapping of *Monkey K9* for the implantation of stimulating electrodes. **A1)** Top view of the monkey brain. Gray parts indicate mapped areas in 2 and 3. **A2, A3)** Mapping of the supplementary motor area (SMA) and primary motor cortex (MI), respectively. Each letter indicated the somatotopic body part: D, digit; E, elbow; H, hip; K, knee; L, lip; J, jaw; S, shoulder; Tr, trunk; W, wrist. Somatotopic arrangements in the mesial surface and the anterior bank of the central sulcus are also shown, along with depth from the cortical surface. Three pairs of bipolar-stimulating electrodes were implanted into the loci, indicated by small gray circles: the forearm region of the SMA and the proximal (MIp) and distal (MId) forelimb regions of the MI. **B)** Schematic representation of the experimental setup. Bipolar stimulating electrodes were chronically implanted in the forelimb regions of the SMA, MIp, and MId. The recording elgiloy electrode with two silica tubes (outside diameter, 147 μm; inside diameter, 74 μm) for microinjection was introduced into the subthalamic nucleus (STN). The Hamilton microsyringe (Teflon-coated tungsten wire with 31-gauge needle; outside diameter, 500 μm) for drug injection was inserted into the striatum (putamen) and the external segment of globus pallidus (GPe) in some experiments.

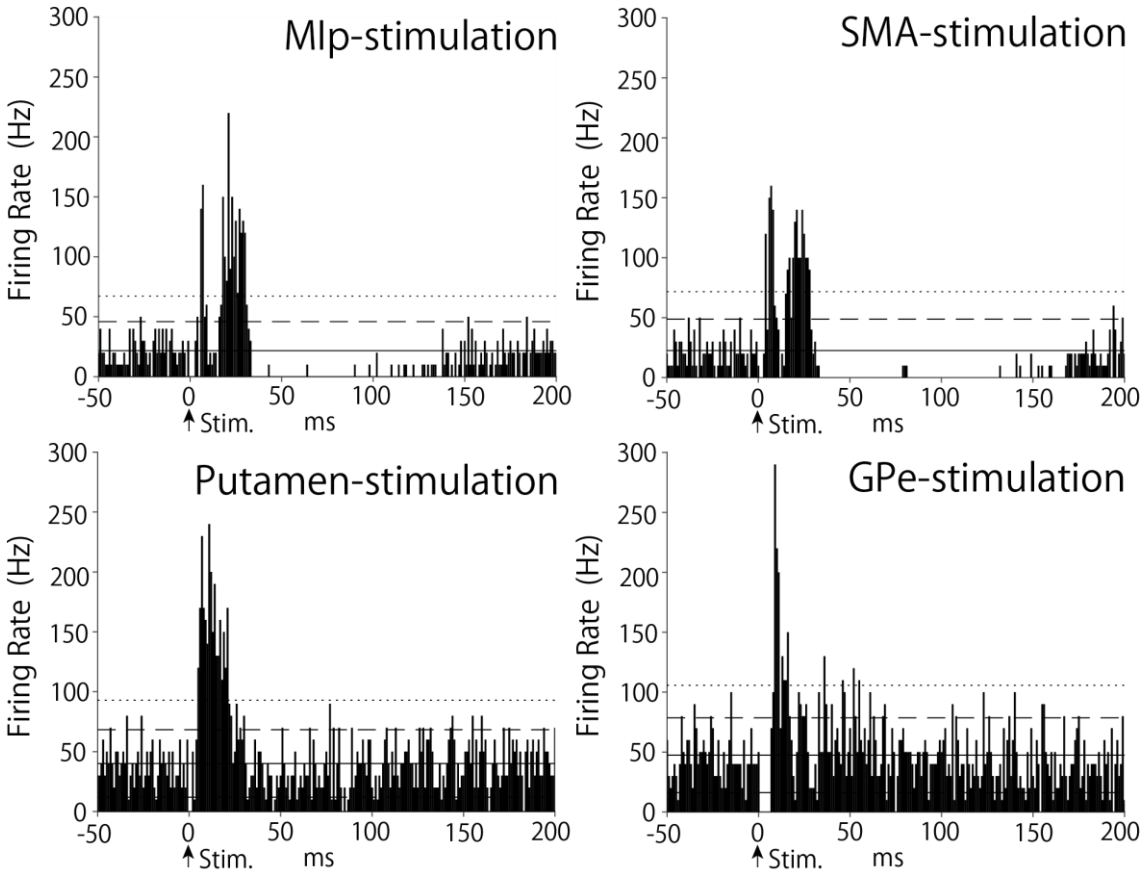

Figure 3. Peristimulus time histograms (PSTHs) of STN neurons in response to MIp, SMA, putamen and GPe stimulations.

PSTHs (100 trials) were constructed in response to the single-pulse stimulation (0.5 mA, arrow-head). Mean, mean ± 1.65 SD ($p < 0.05$, one-tailed *t*-test), and mean ± 3.09 SD ($p < 0.001$, one-tailed *t*-test) were indicated by solid (mean), dashed (mean ± 1.65 SD), and dotted (mean ± 3.09 SD) lines, respectively.

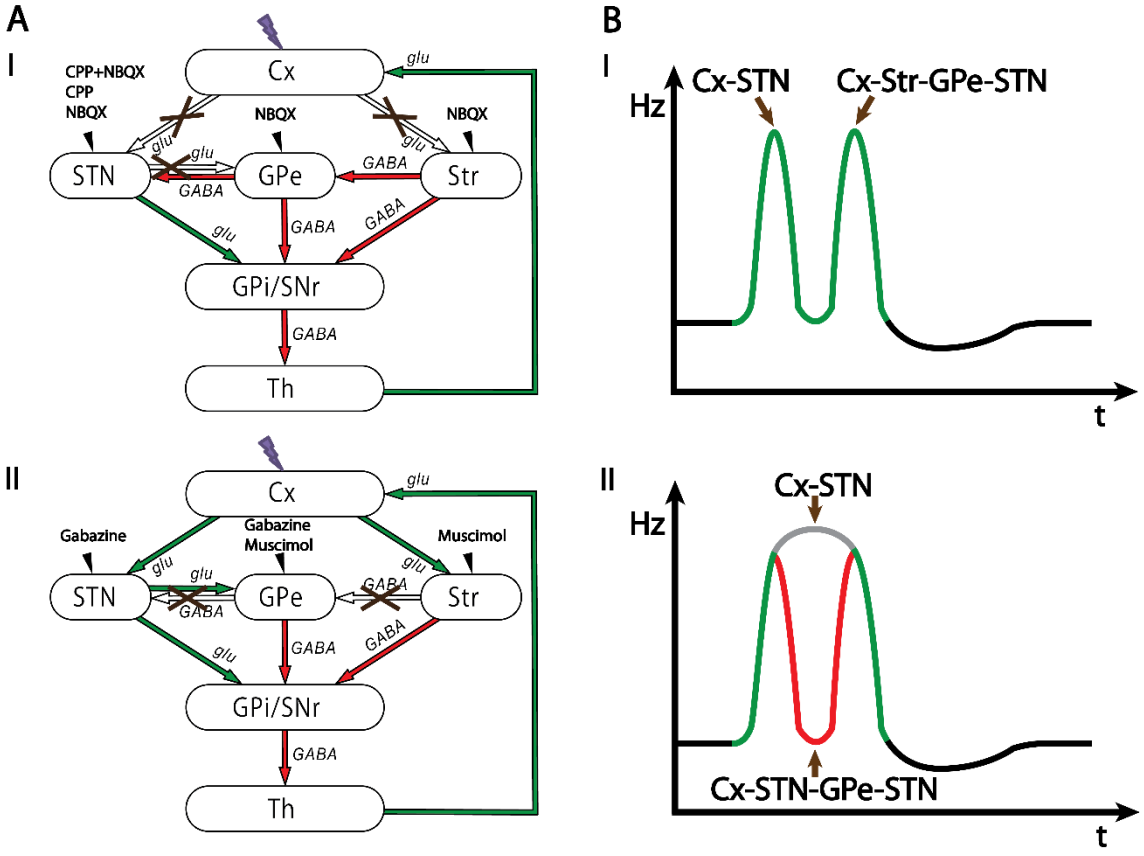

Figure 4. Method and hypotheses of the study.

A) Basic circuitry of the basal ganglia (BG). Green and red arrows represent excitatory glutamatergic (glu) and inhibitory GABAergic (GABA) projections, respectively. White arrow with cross mark represents blockade of signal transmission. Purple lightning mark represents the area of electrical stimulation. I) STN neurons receive glutamatergic inputs from the cortex via the *hyperdirect* pathway. Local injection of CPP and NBQX blocks these glutamatergic inputs. II) STN neurons receive cortical inputs via the *indirect* pathway through the striatum and GPe. Muscimol injection into the striatum, and gabazine or muscimol injection into the GPe block this pathway. STN neurons finally receive GABAergic inputs from the GPe. Local injection of gabazine blocks the GABAergic inputs. **B)** Two possible origins of cortically evoked biphasic responses in the STN. ***I)*** Early and late excitations are mediated by the *hyperdirect* and *indirect*

pathways (green lines), respectively; ***II)*** Cortically induced long excitation (gray line) is intervened by the inhibition from the GPe (red line). Cx, cerebral cortex; STN, subthalamic nucleus; GPe, external segment of globus pallidus; Str, striatum; GPi, internal segment of globus pallidus; SNr substantia nigra pars reticulata; Th, thalamus.

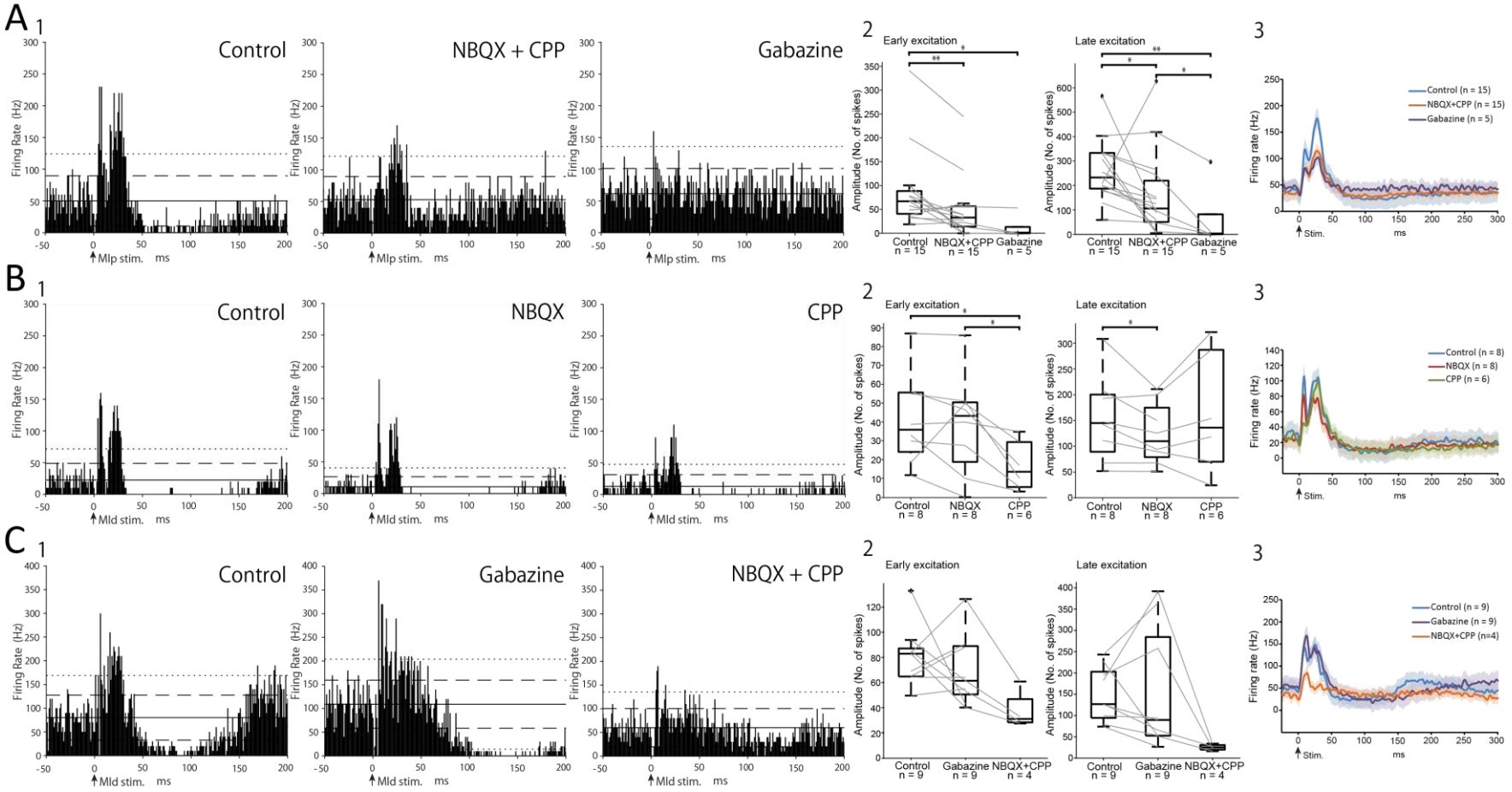
A
1
Control
NBQX + CPP
Gabazine
Firing Rate (Hz)
MIp stim.
ms
2
Early excitation
Late excitation
Amplitude (No. of spikes)
Control n = 15
NBQX+CPP n = 15
Gabazine n = 5
3
Control (n = 15)
NBQX+CPP (n = 15)
Gabazine (n = 5)
Firing rate (Hz)
Stim.
B
1
Control
NBQX
CPP
MId stim.
2
Control n = 8
NBQX n = 8
CPP n = 6
3
Control (n = 8)
NBQX (n = 8)
CPP (n = 6)
C
1
Control
Gabazine
NBQX + CPP
2
Control n = 9
Gabazine n = 9
NBQX+CPP n = 4
3
Control (n = 9)
Gabazine (n = 9)
NBQX+CPP (n=4)

Figure 5

Figure 5. Cortically evoked responses of STN neurons after local drugs injections into the STN.

Changes in biphasic response evoked by cortical stimulation before and after drugs injections in the following order into the STN: **A)** NBQX+CPP, then gabazine; **B)** NBQX, then CPP; **C)** Gabazine, then NBQX + CPP. **A1, B1, C1:** PSTHs in response to cortical stimulation (arrow-head, single-pulse stimulation, 0.5 mA, 100 times). **A2, B2, C2:** Quantitative analyses of amplitudes of early and late excitations before and after drugs injections. *$p < 0.05$, **$p < 0.01$, paired, one-tailed t-test. **A3, B3, C3:** Population PSTHs of STN neurons. Data obtained before (blue) and after NBQX+CPP (orange), NBQX (red-orange), CPP (green), gabazine (purple) injections. The light shaded colors represent ± SD.

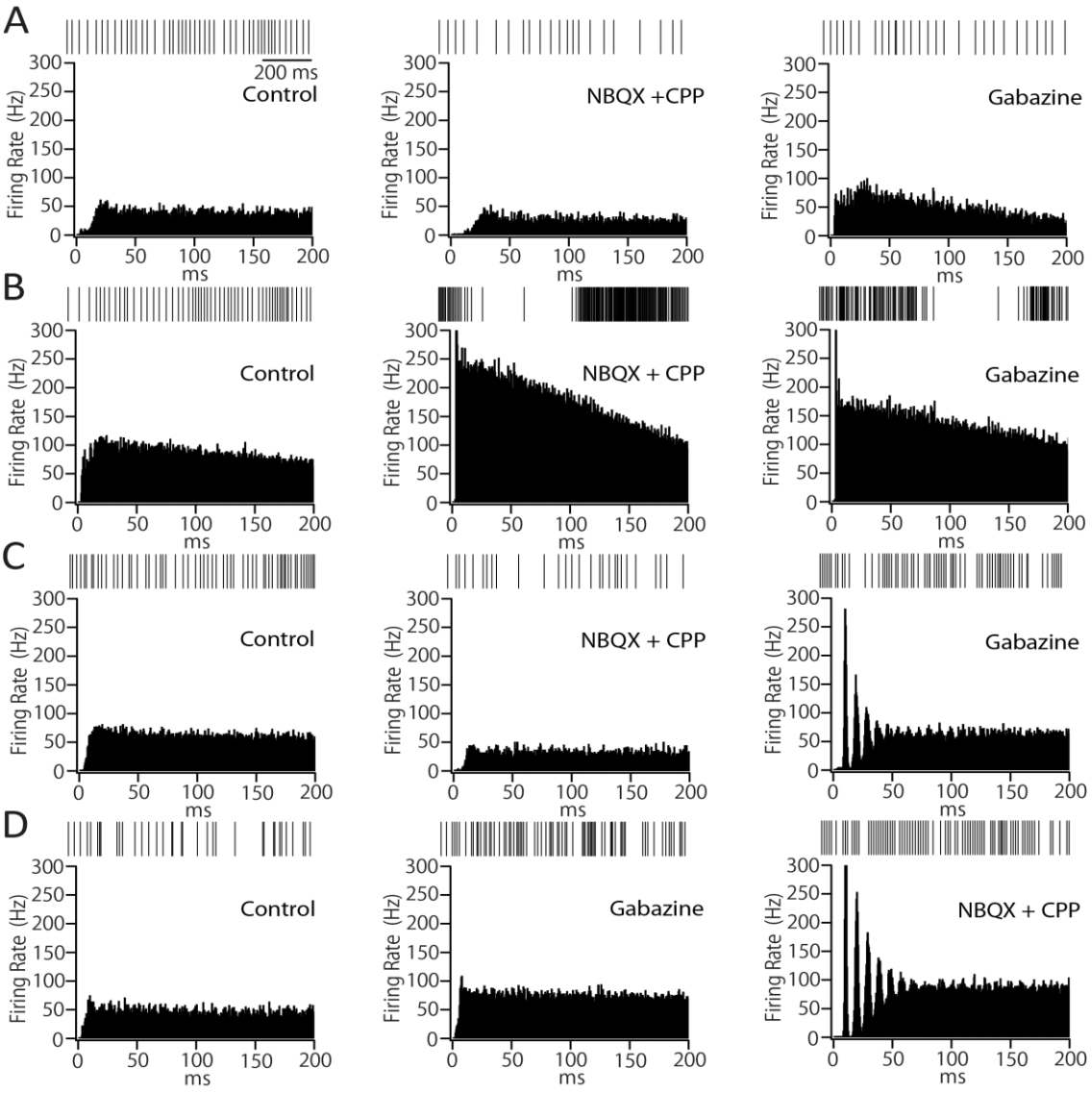

Figure 6. Spontaneous activity of STN neurons before and after drugs injections in the vicinity of recorded units.

Digitized spikes (top) and autocorrelograms (bottom) of spontaneous activity of STN neurons are shown before and after drugs injections in the following order: **A-C)** NBQX + CPP, then gabazine; **D)** Gabazine, then NBQX+CPP.

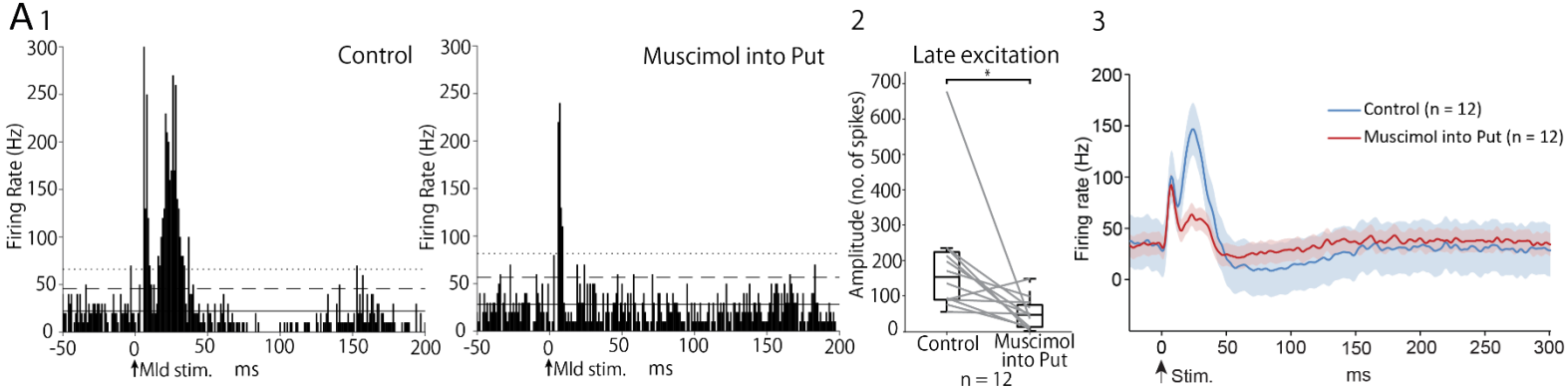

Figure 7. Cortically evoked responses of STN neurons after blockade of the putamen.

A1: PSTHs in response to cortical stimulation (arrow-head, single-pulse stimulation, 0.5 mA, 100 times) before and after injection of muscimol into the putamen. **A2:** Quantitative analyses of amplitudes of late excitations before and after muscimol injection. *$p < 0.05$, **$p < 0.01$, paired, one-tailed t-test. **A3:** Population PSTHs of STN neurons. Data obtained before (blue) and after muscimol (magenta) injections.

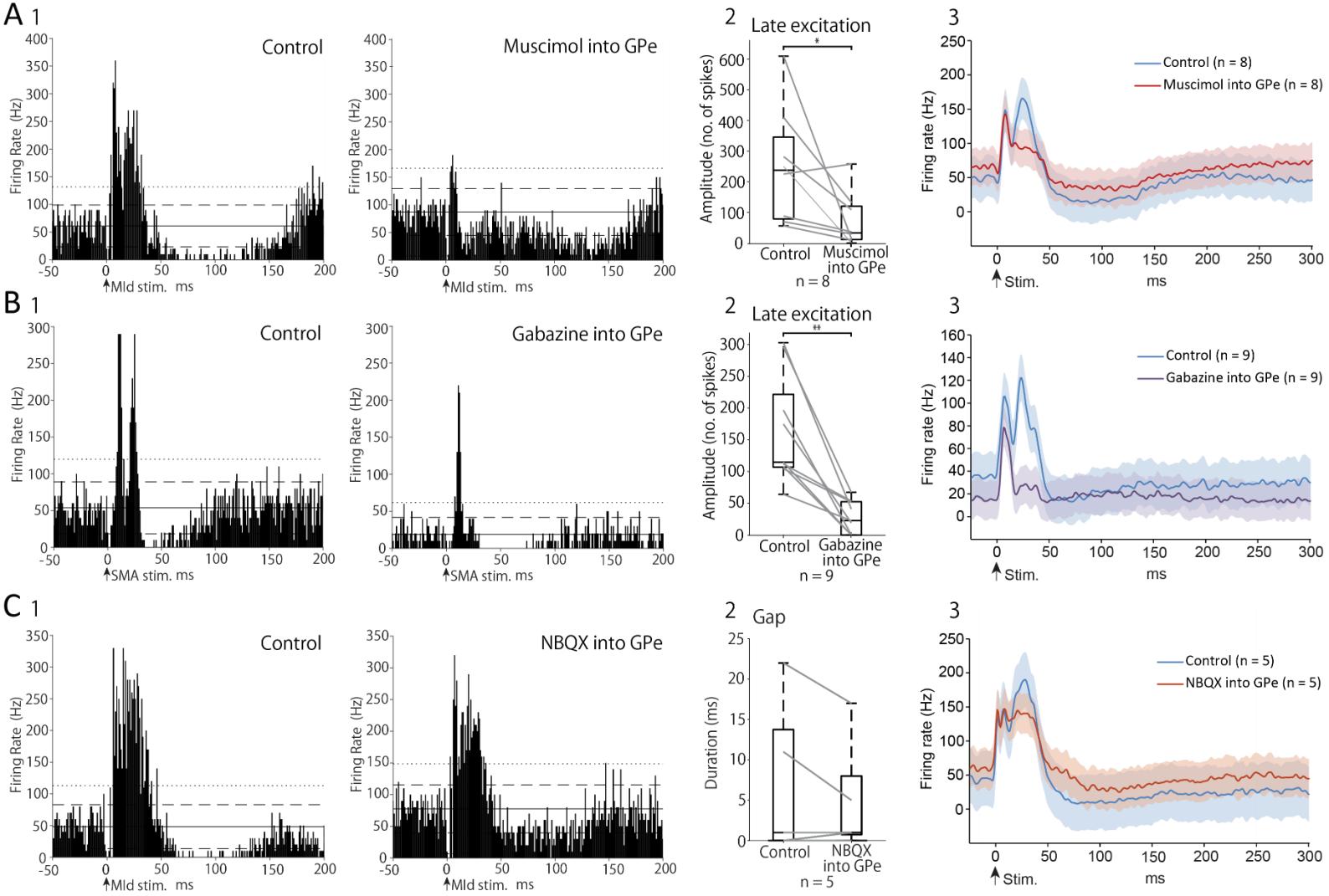
A
1
Control
Muscimol into GPe
Firing Rate (Hz)
MId stim. ms
2
Late excitation
Amplitude (no. of spikes)
Control
Muscimol into GPe
n = 8
3
Control (n = 8)
Muscimol into GPe (n = 8)
Firing rate (Hz)
Stim.
ms
B
1
Control
Gabazine into GPe
SMA stim. ms
2
Late excitation
Gabazine into GPe
n = 9
3
Control (n = 9)
Gabazine into GPe (n = 9)
C
1
Control
NBQX into GPe
2
Gap
Duration (ms)
NBQX into GPe
n = 5
3
Control (n = 5)
NBQX into GPe (n = 5)

Figure 8

Figure 8. Cortically evoked responses of STN neurons after blockade of the GPe.

Changes in the biphasic response of the STN neurons evoked by cortical stimulation after blockade of the GPe by injecting following drugs: **A)** Muscimol; **B)** Gabazine; **C)** NBQX. **A1, B1, C1:** PSTHs in response to cortical stimulation (arrow-head, single-pulse stimulation, 0.5 mA, 100 times) before and after drug injection into the GPe. **A2, B2:** Quantitative analyses of amplitudes of late excitations before and after drugs injections. *$p < 0.05$, ** $p < 0.01$, paired, one-tailed t-test. **C2:** Quantitative analyses of the gap duration between two excitations before and after NBQX injection. **A3, B3, C3:** Population PSTHs of STN neurons. Data obtained before (blue) and after muscimol (magenta), gabazine (purple), NBQX (red-orange) injections.

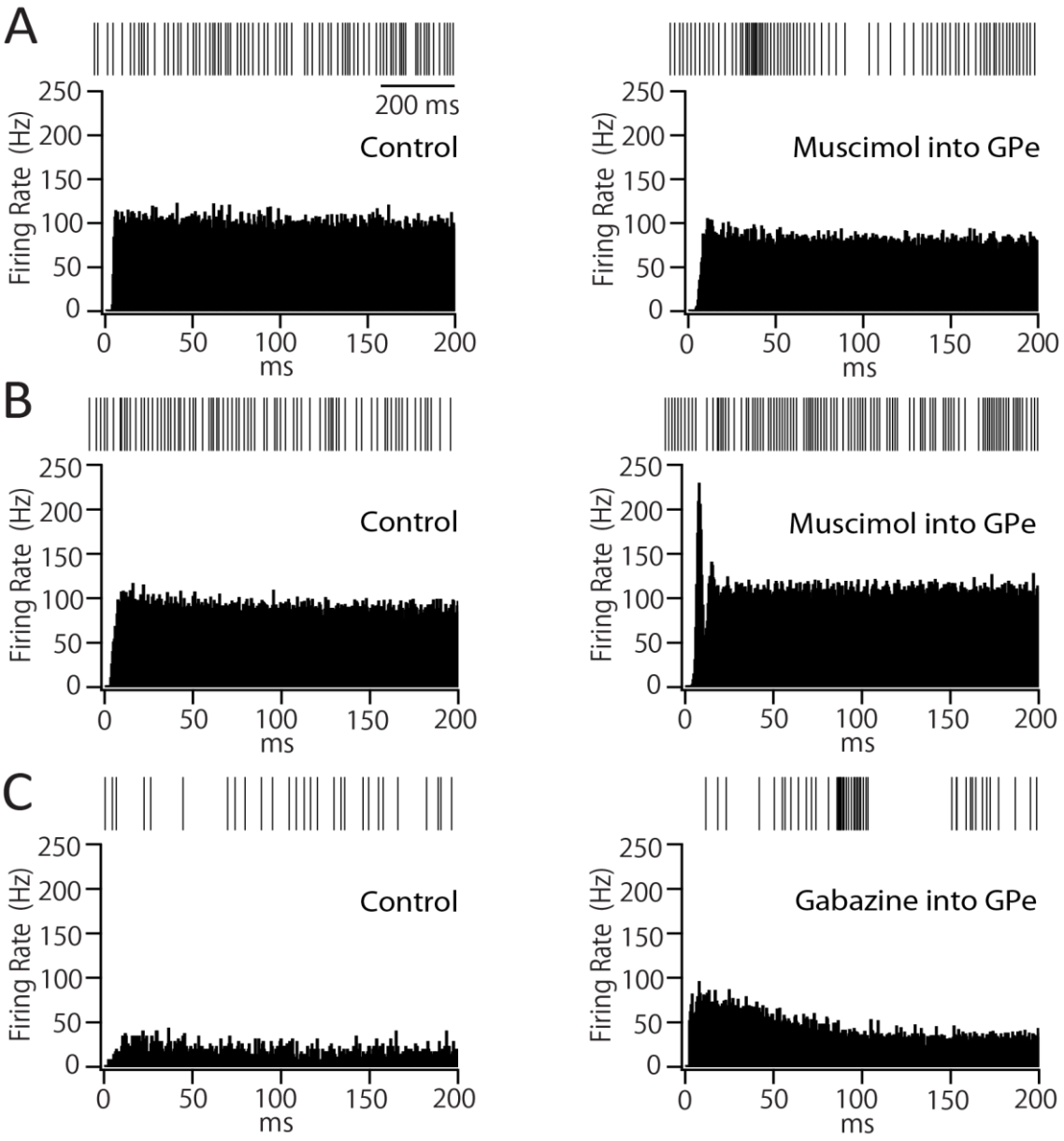

Figure 9. Spontaneous activity of STN neurons before and after drugs injections into the GPe.

Digitized spikes (top) and autocorrelograms (bottom) of spontaneous activity of STN neurons are shown before and after the injections of the following drug into the GPe: **A-B)** Muscimol; **C)** Gabazine.

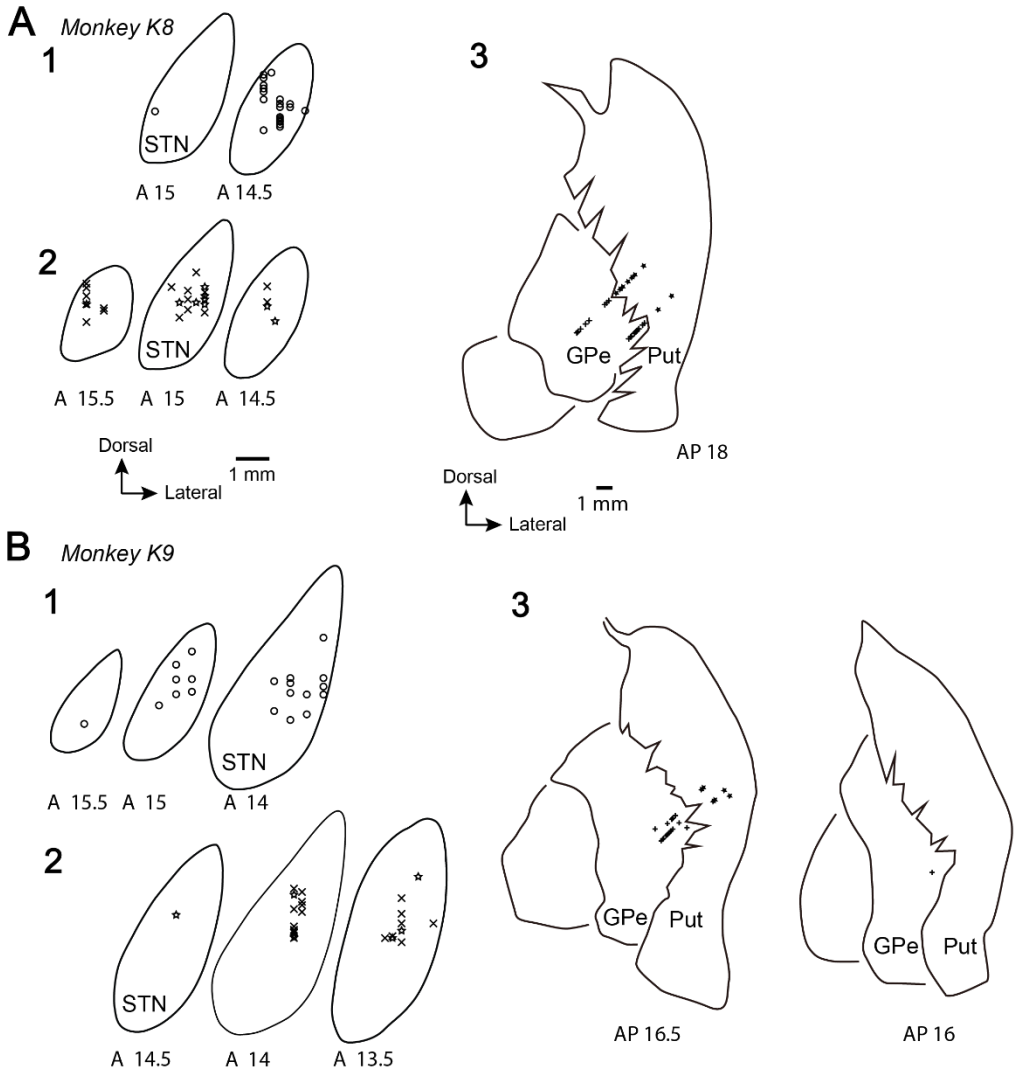
A
Monkey K8
1
STN
A 15
A 14.5
2
STN
A 15.5
A 15
A 14.5
Dorsal
Lateral
1 mm
3
GPe
Put
AP 18
Dorsal
Lateral
1 mm
B
Monkey K9
1
STN
A 15.5
A 15
A 14
2
STN
A 14.5
A 14
A 13.5
3
GPe
Put
AP 16.5
GPe
Put
AP 16

Figure 10

Figure 10. Locations of recorded STN neurons and drug injection sites in the putamen and GPe in *Monkey K8* (left hemisphere) **(A)** and *Monkey K9* (right hemisphere) **(B). A1, B1:** Locations of recorded STN neurons (circle) with drugs injections in the vicinity of recorded neurons. **A2, B2:** Location of recorded STN neurons with drugs injections into the putamen (star) or GPe (cross). **A3, B3:** Locations of injection into the putamen (starts) and GPe (crosses).

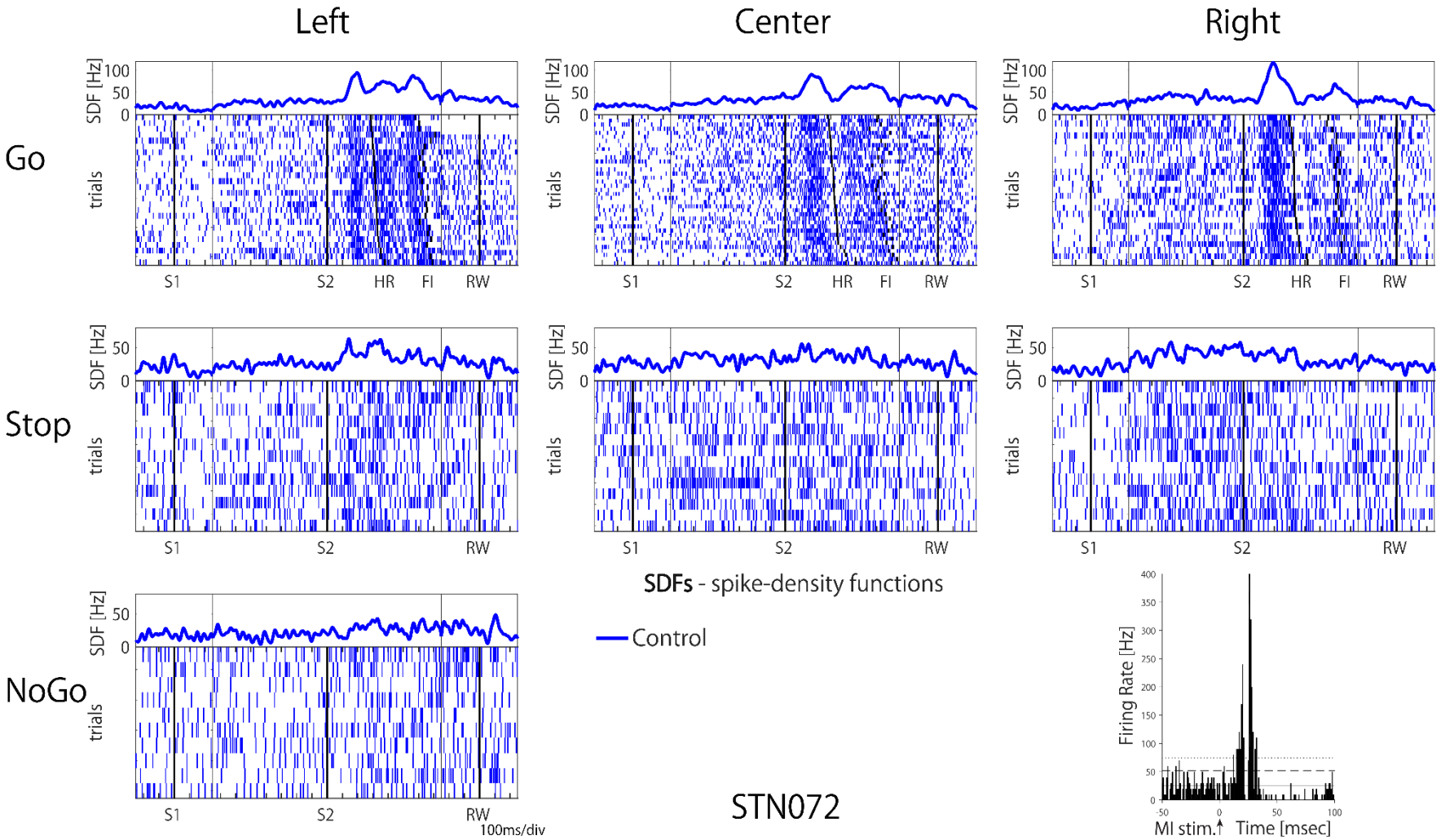
Left
Center
Right
Go
Stop
NoGo
SDF [Hz]
trials
S1
S2
HR
FI
RW
100ms/div
SDFs - spike-density functions
Control
STN072
Firing Rate [Hz]
MI stim.
Time [msec]

Figure 11

Figure 11. STN activity during task performance.

Raster plots demonstrate the neuronal firings (blue vertical lines) during the performance of goal-directed reaching task with delay. Neuronal activity was aligned separately according to the instruction signal (S1), triggering signal (S2) and reward (RW) events in all types of trials (Go, Stop, NoGo) and target directions (Left, Center, Right). Each plot of "Go" trials was sorted according to the reaction time (S2-HR). Continuous blue traces indicate spike density functions (SDFs, σ = 10 ms) for associated raster plots. PSTHs in the bottom-right corner showed the response to cortical stimulation (1 ms bin, summed for 100 stimuli, 300 µs duration, single pulse, strength of 0.5 mA and interval of 1.4 s).

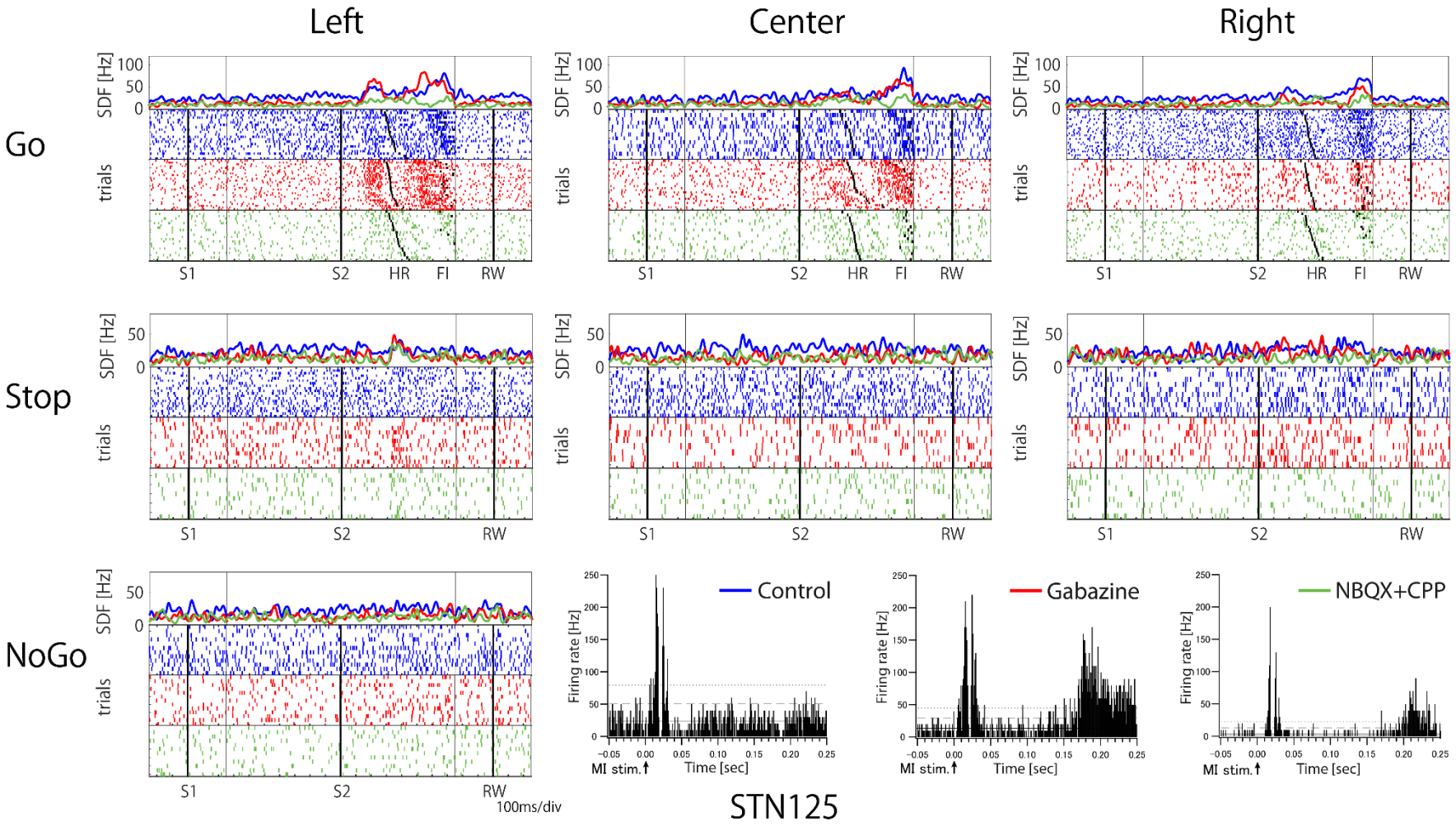
Left
Center
Right
Go
Stop
NoGo
SDF [Hz]
trials
S1
S2
HR
FI
RW
100ms/div
Control
Gabazine
NBQX+CPP
Firing rate [Hz]
MI stim.
Time [sec]
STN125

Figure 12

Figure 12. Raster plots and SDFs during the performance of goal-directed reaching task with delay in the control state (blue) and after local gabazine injection (red) followed by NBQX+CPP injection (green) into the STN. PSTHs of responses evoked by cortical stimulation in the bottom of the figure.

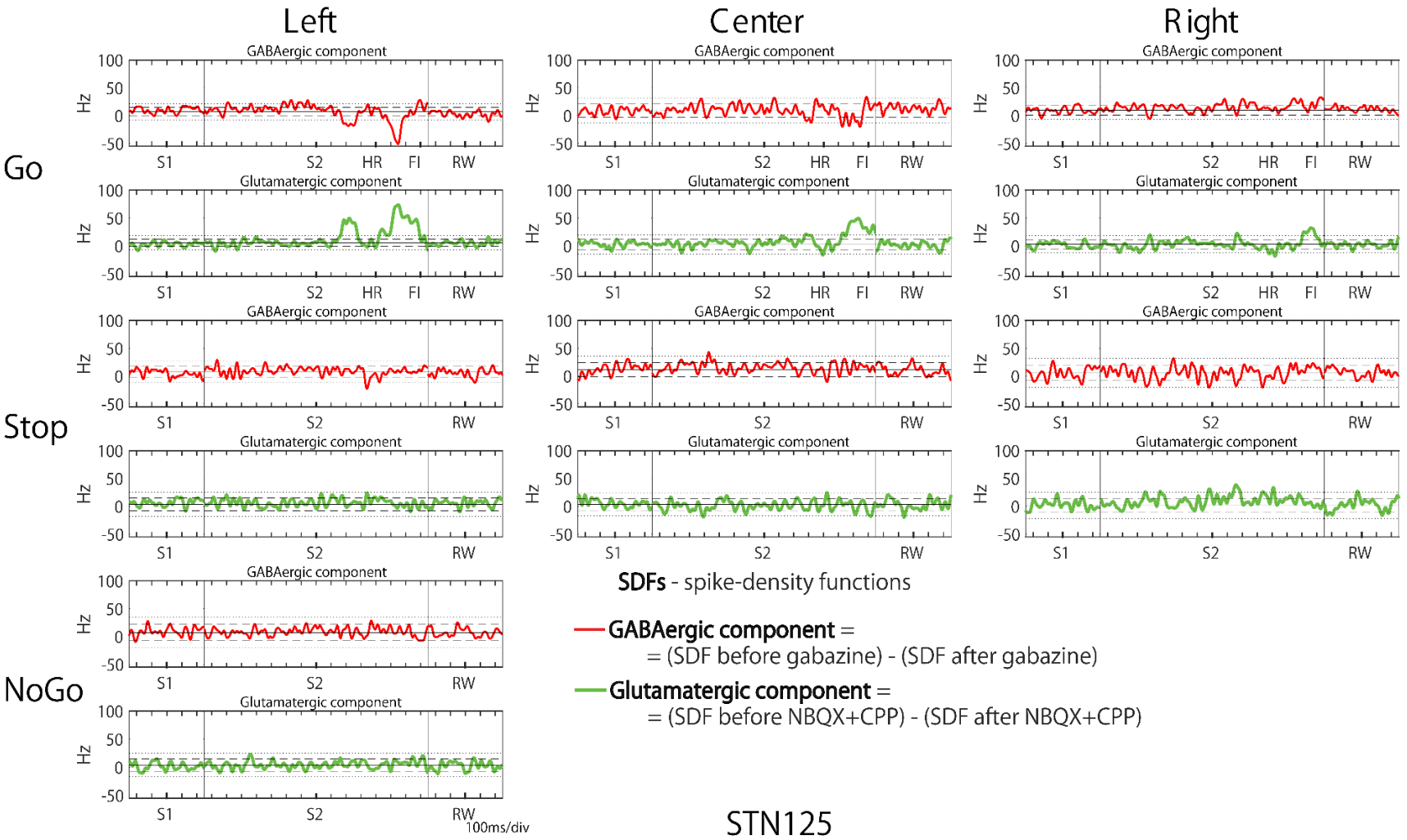

Figure 13. GABAergic (red) and glutamatergic (green) components of the STN neuron indicated in Figure 12 during task performance.

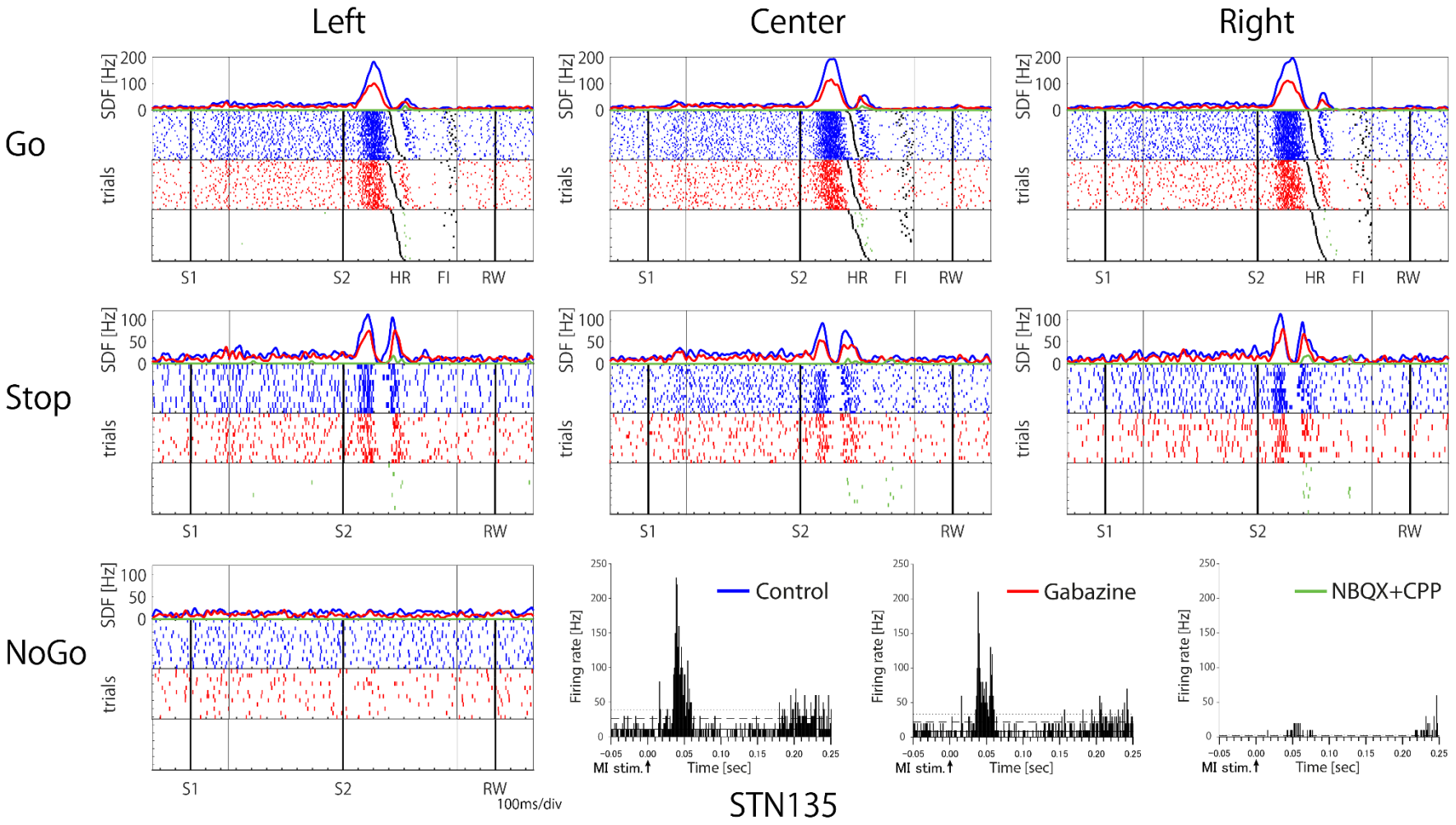

Figure 14. Another example of STN activity during task performance.

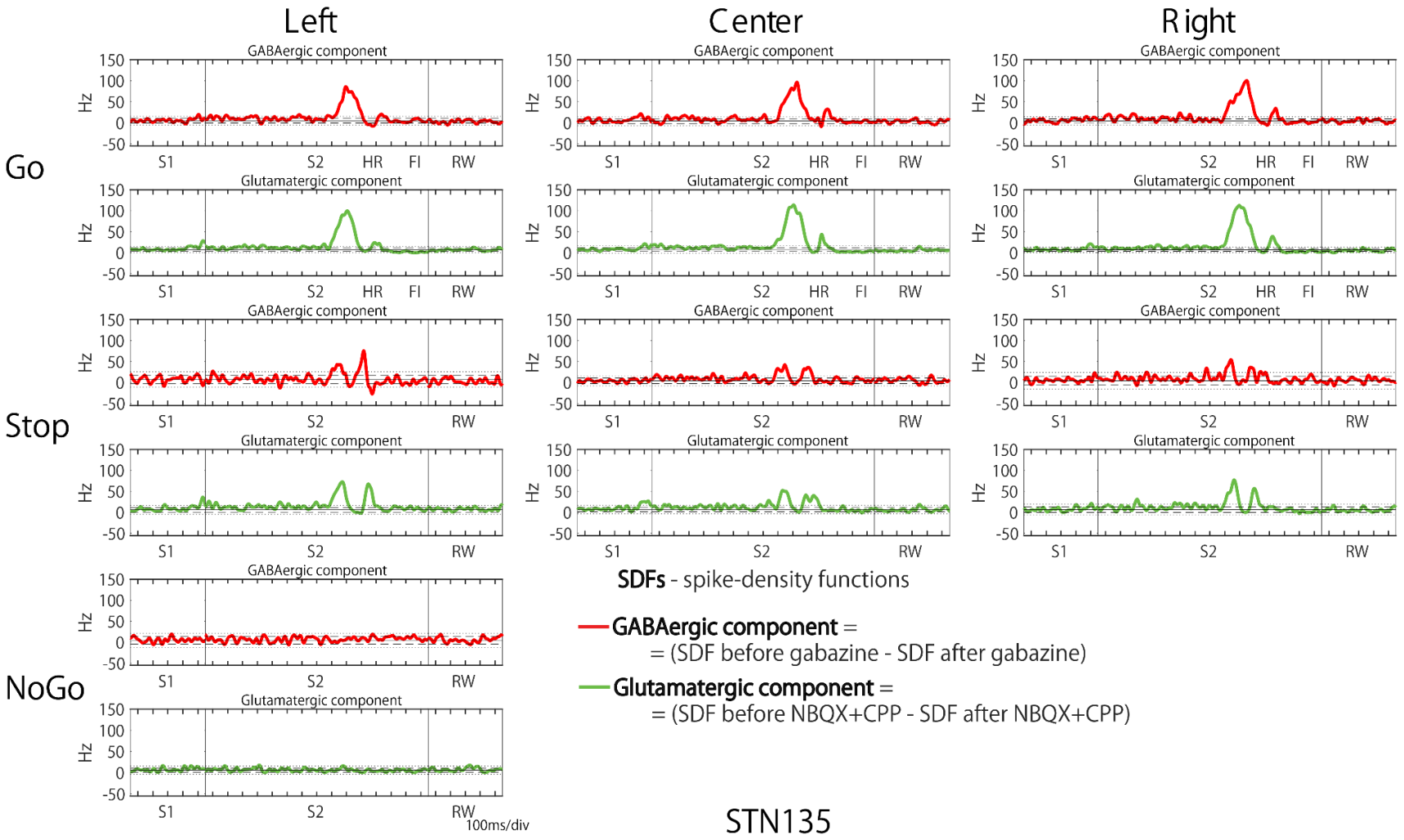

Figure 15. GABAergic and glutamatergic components of the STN neuron indicated in Figure 14 during task performance.

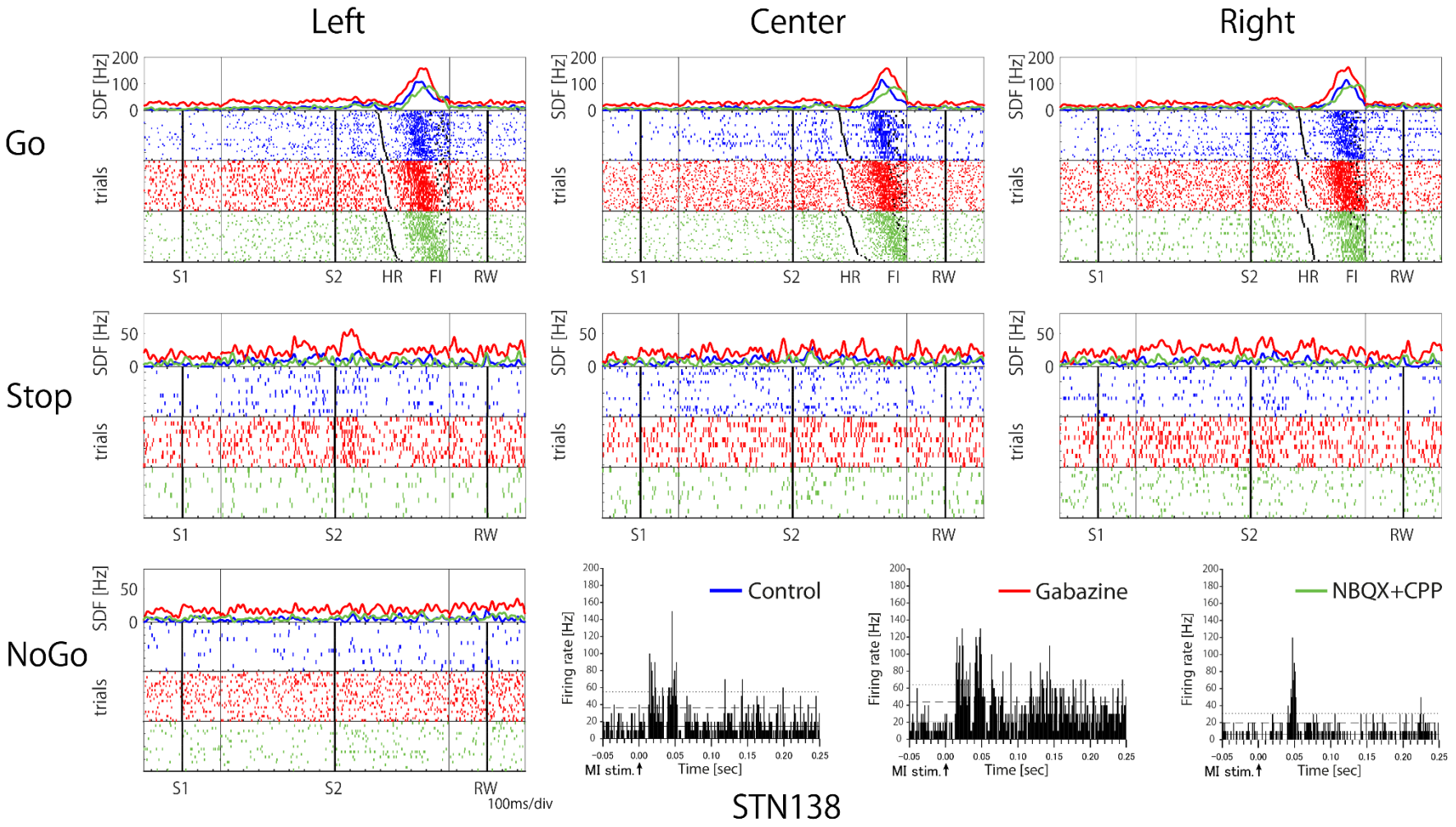

Figure 16. Another example of STN activity during task performance.

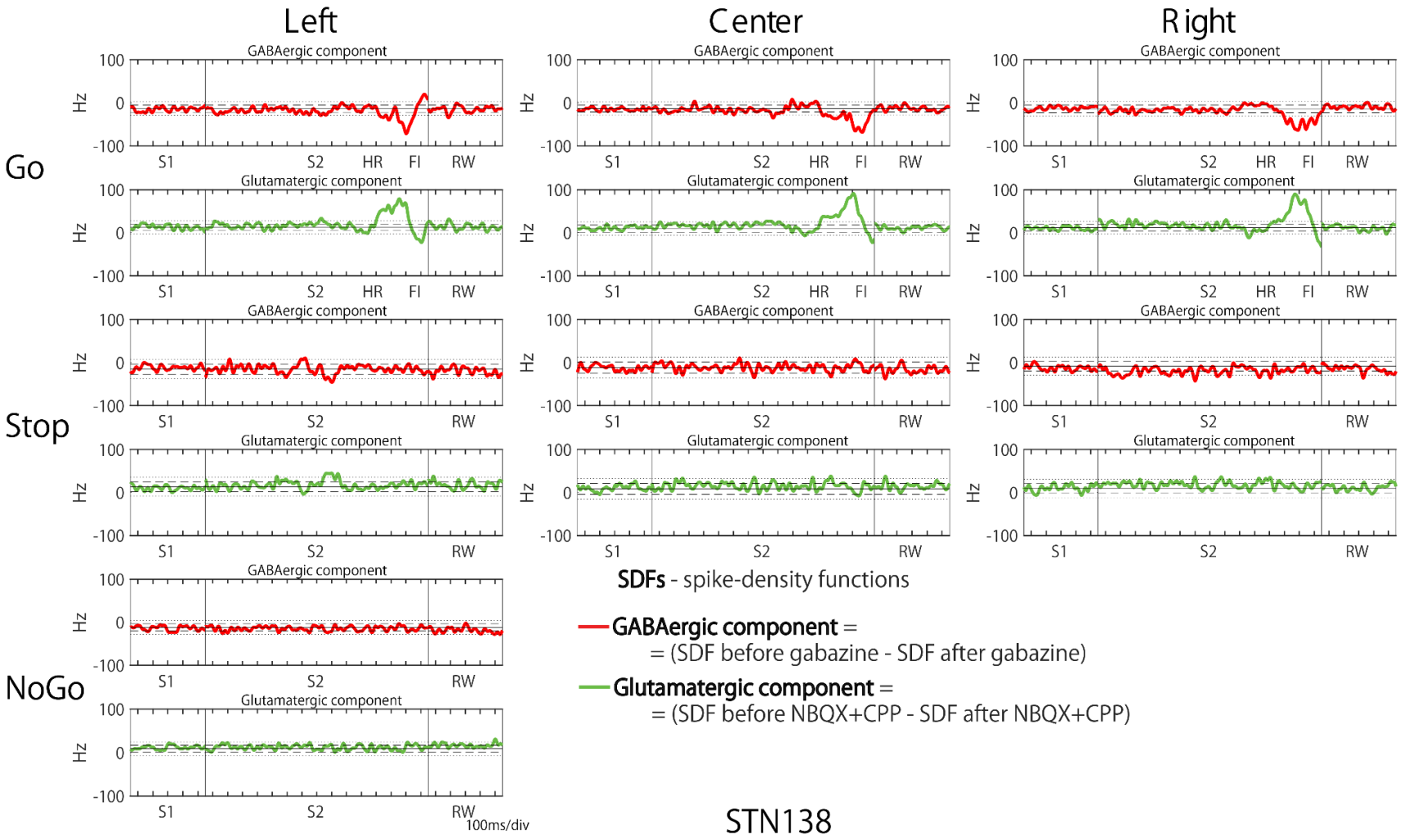

Figure 17. GABAergic and glutamatergic components of the STN neuron indicated in Figure 16 during task performance.

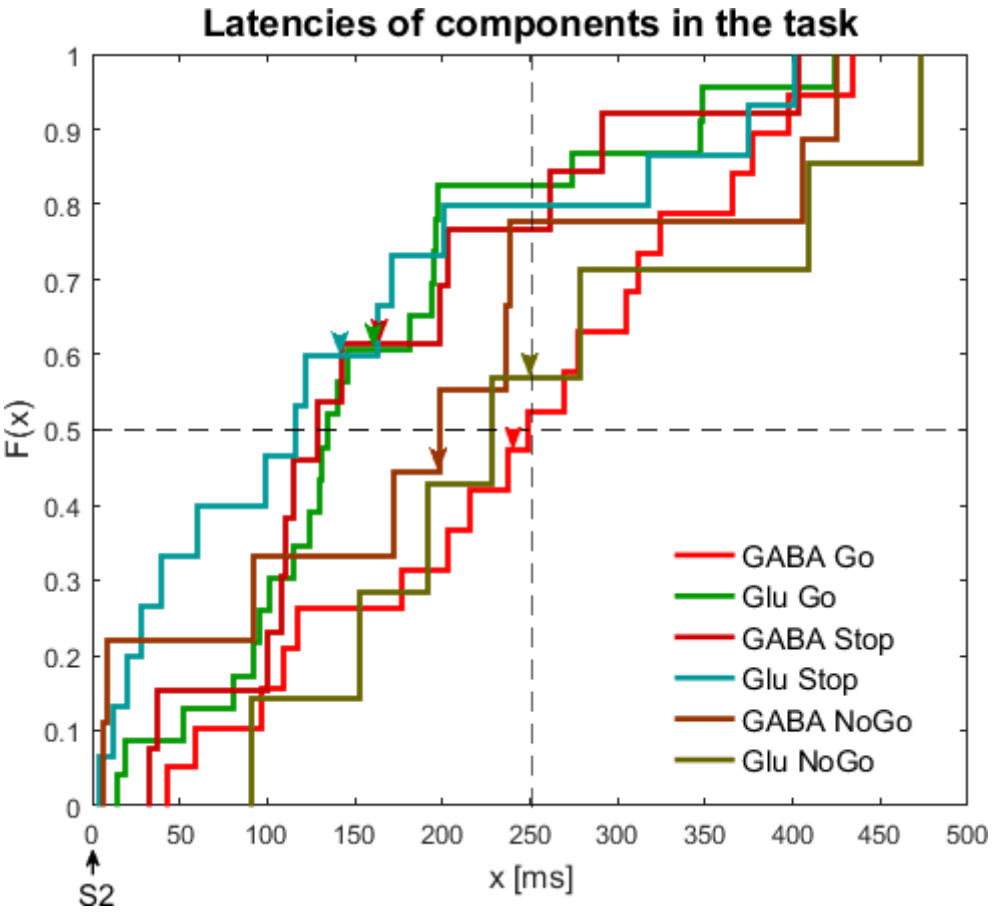

Figure 18. Cumulative histograms showing latencies of GABAergic (GABA) and glutamatergic (Glu) components in Go, Stop, and NoGo trials of goal-directed reaching task with delay.

Arrowheads indicate the mean latencies. Latencies of GABAergic and glutamatergic components in "Go" trials were significantly different ($p = 0.0178$, one-tailed paired *t*-test).

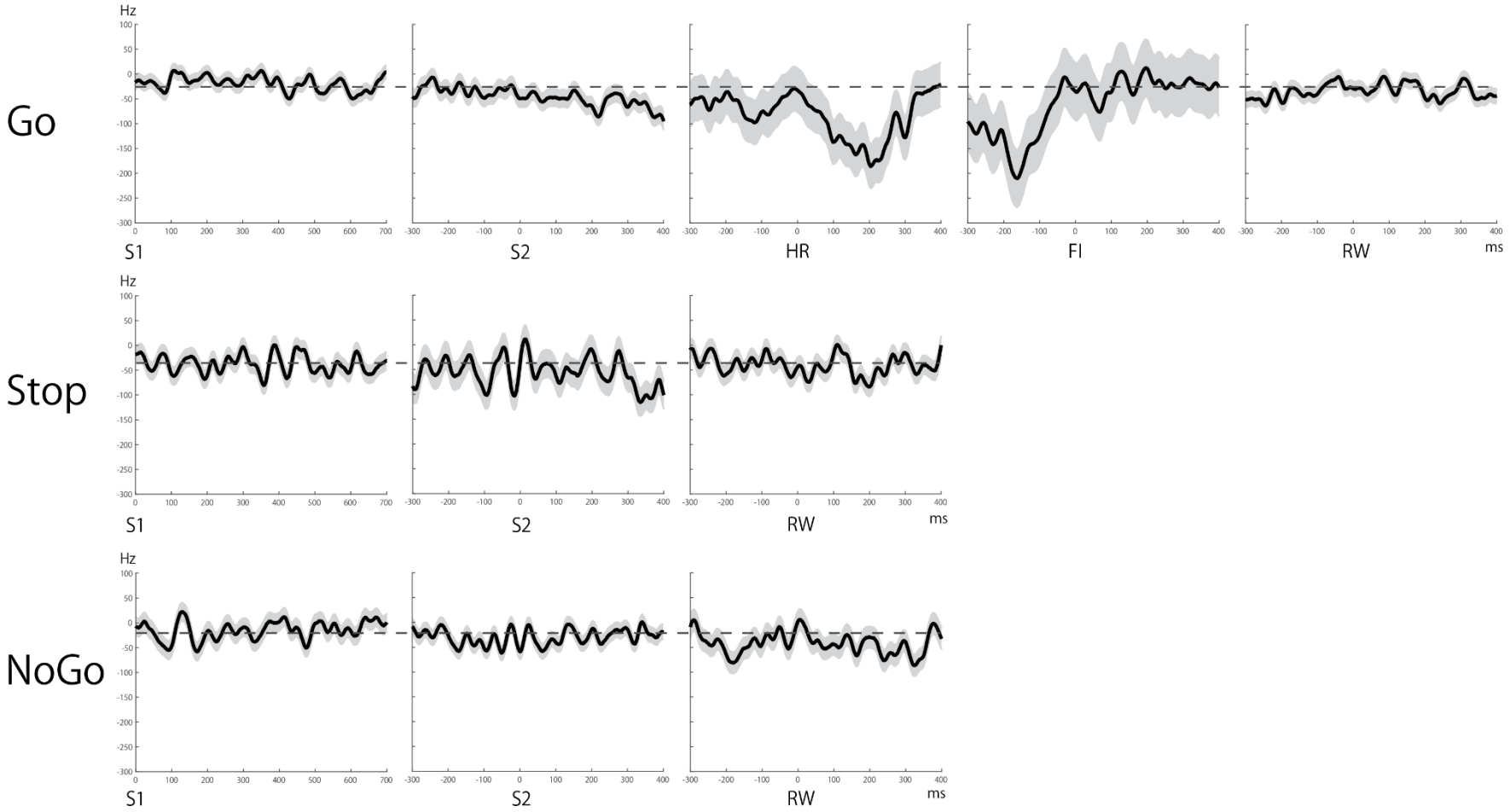

Figure 19. Population activity of GABAergic component of STN neurons with inhibitory GABAergic and facilitatory glutamatergic components (n = 9, 39%). Grey shaded area indicates SD and the dotted line shows the mean calculated within 1000ms before S1 event.

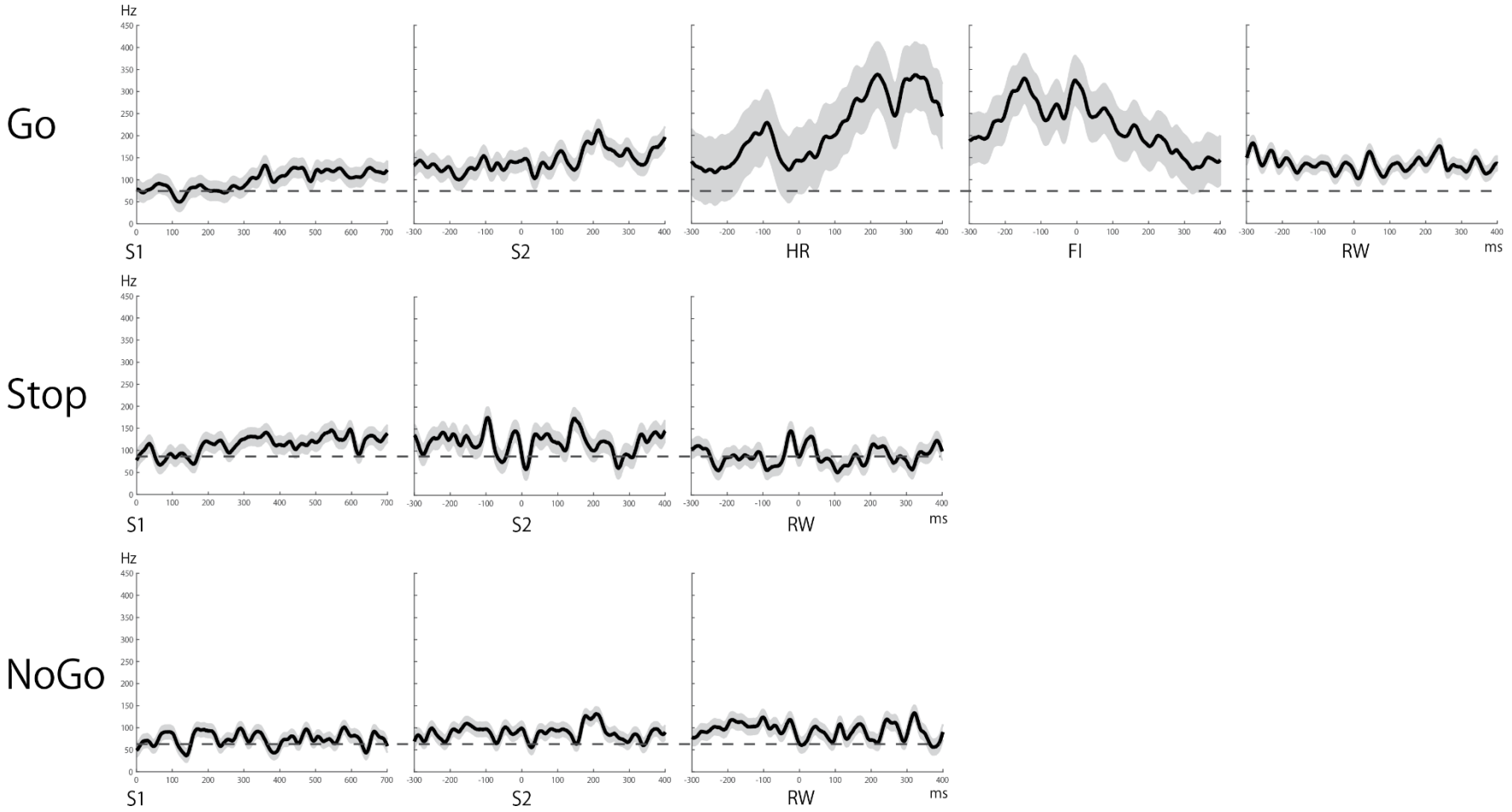

Figure 20. Population activity of glutamatergic component of STN neurons with inhibitory GABAergic and facilitatory glutamatergic components (n = 9, 39%).

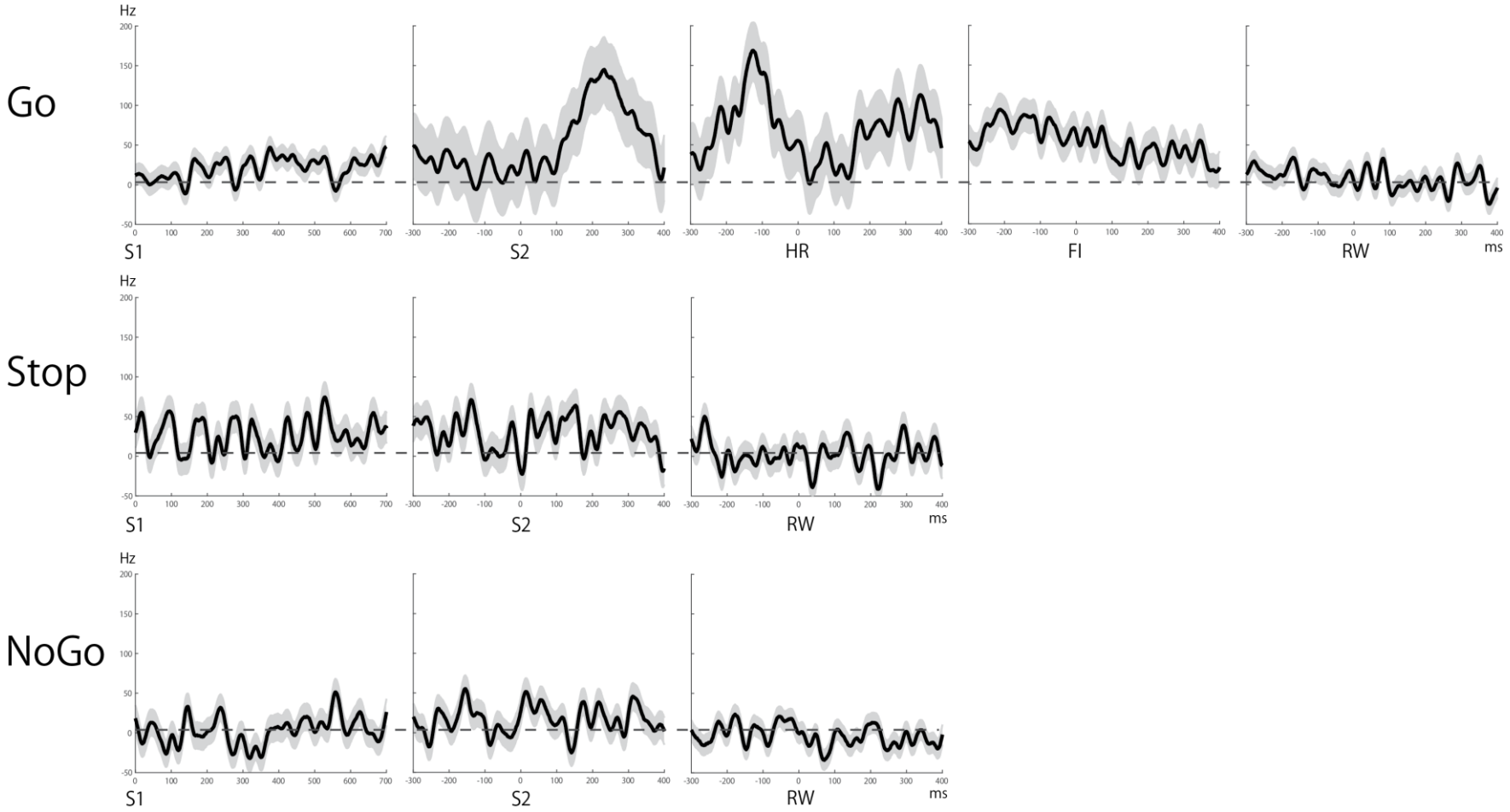

Figure 21. Population activity of GABAergic component of STN neurons with facilitatory GABAergic and facilitatory glutamatergic components (N=8, 35%).

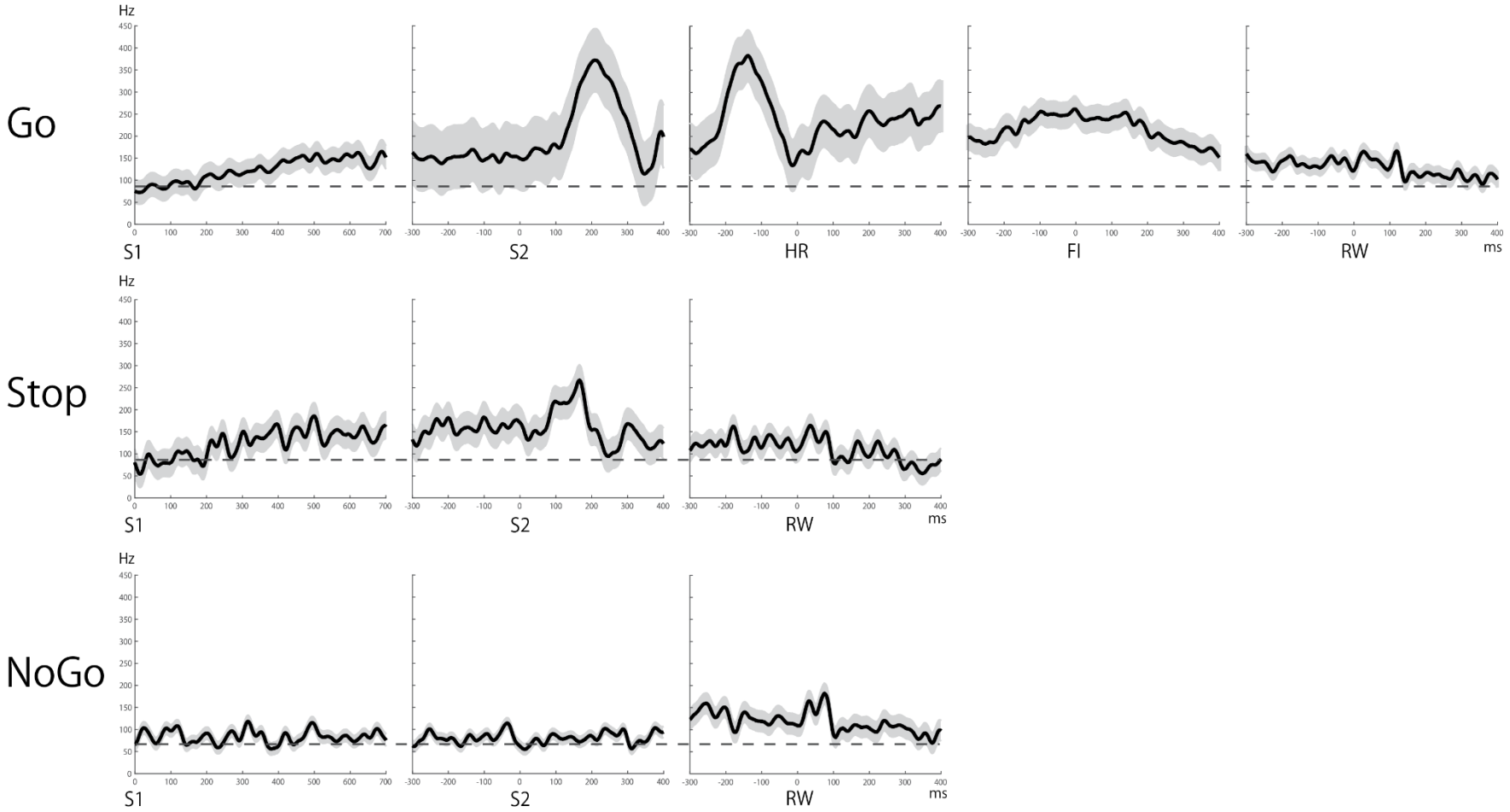

Figure 22. Population activity of glutamatergic component of STN neurons with facilitatory GABAergic and facilitatory glutamatergic components (N=8, 35%).

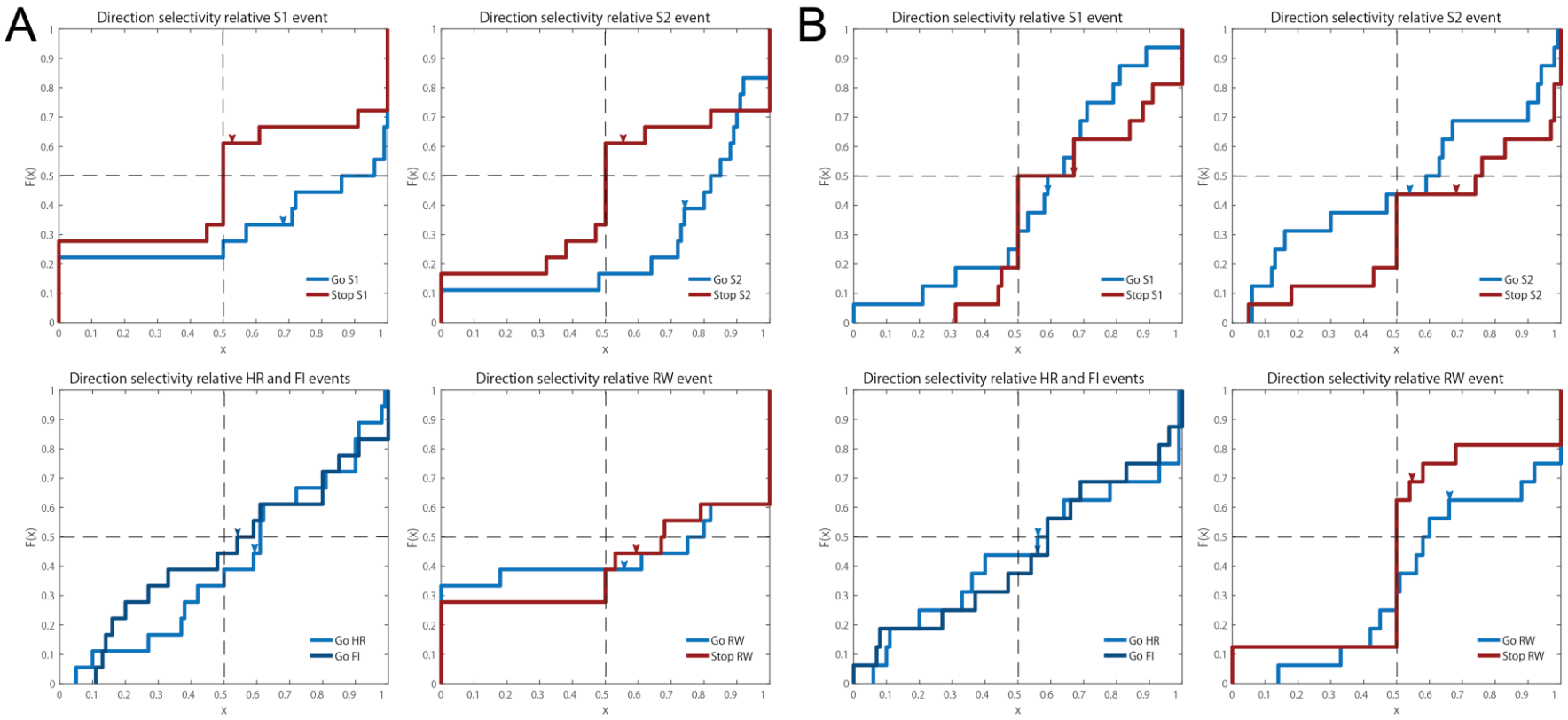
A
Direction selectivity relative S1 event
Go S1
Stop S1
Direction selectivity relative S2 event
Go S2
Stop S2
Direction selectivity relative HR and FI events
Go HR
Go FI
Direction selectivity relative RW event
Go RW
Stop RW
B
Direction selectivity relative S1 event
Go S1
Stop S1
Direction selectivity relative S2 event
Go S2
Stop S2
Direction selectivity relative HR and FI events
Go HR
Go FI
Direction selectivity relative RW event
Go RW
Stop RW
F(x)
x

Figure 23

Figure 23. Cumulative histograms showing DS at task events.

The comparison was performed between “Go” (blue color) and “Stop” (dark red color) trials at S1, S2, HR, FI RW task events. **A)** DS calculated from STN neurons with that showed inhibitory GABAergic and facilitatory glutamatergic components. In “Go” trials, DS at S2 was 0.74±0.26 and significantly higher than in “Stop” trials (0.57±0.36; p = 0.018, one-tailed paired *t*-test). **B)** DS calculated from STN neurons with facilitatory GABAergic and facilitatory glutamatergic components.

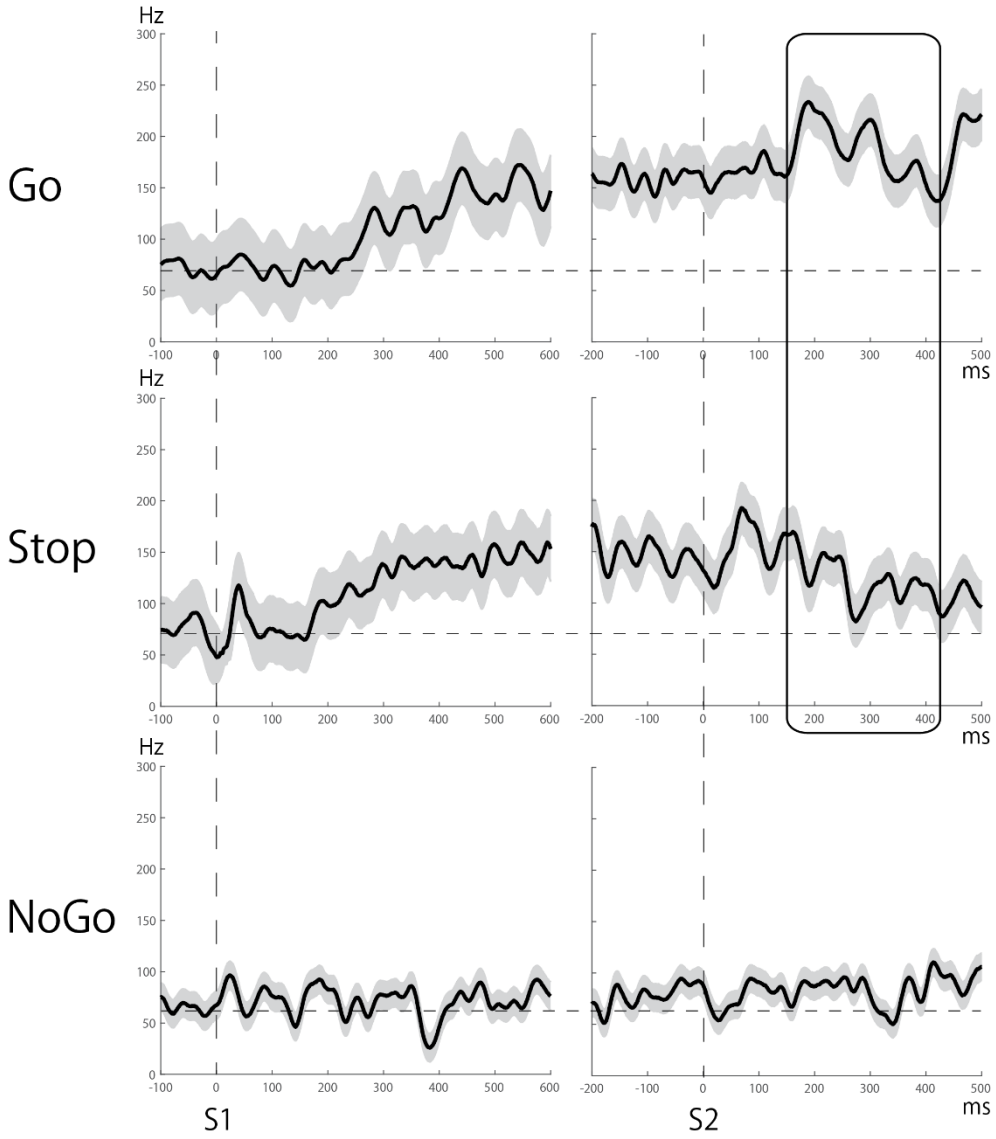

Figure 24. Cumulative activity of glutamatergic component of STN neurons with buildup activity during delay period after S1 (N=7, 30%).

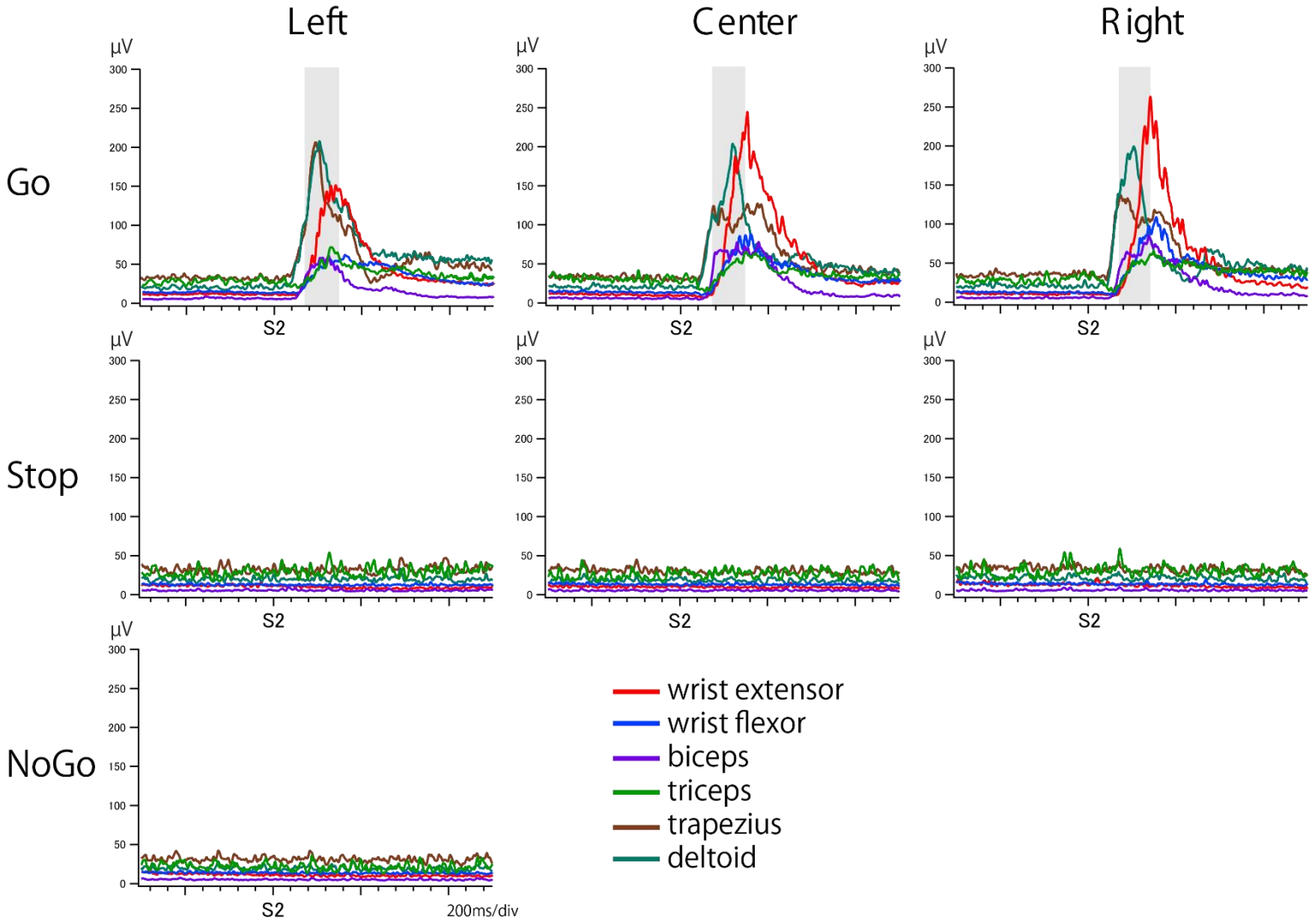
Left
Center
Right
Go
Stop
NoGo
µV
300
250
200
150
100
50
0
S2
200ms/div
wrist extensor
wrist flexor
biceps
triceps
trapezius
deltoid

Figure 25

Figure 25. The example of EMG activity during task performance.

EMG was recorded from wrist extensor, wrist flexor, biceps brachii, triceps brachii, trapezius, and deltoid and aligned with S2 signal. Shaded areas represent the timing of movements.

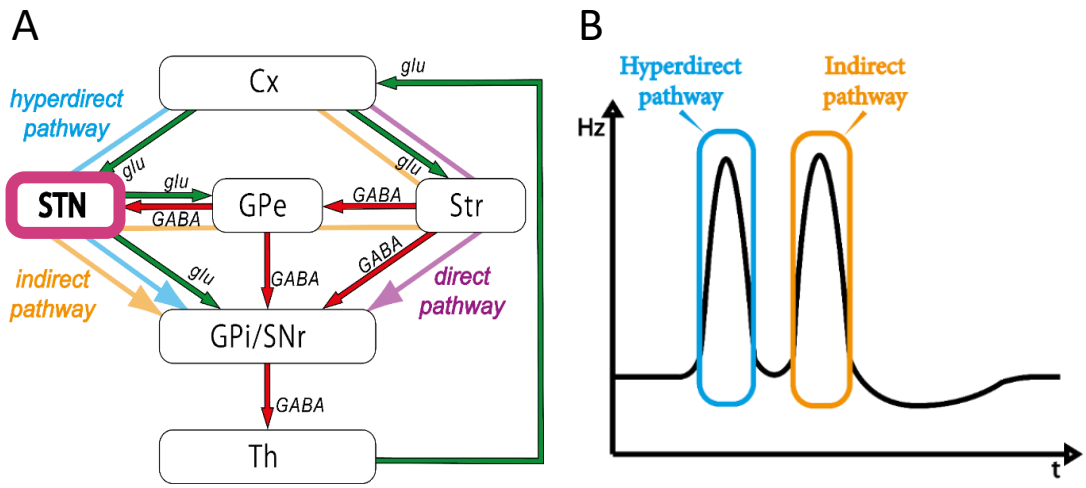

Figure 26. The origin of the STN biphasic response to cortical stimulation.

A) Basic circuitry of the BG. Green and red arrows represent excitatory glutamatergic (glu) and inhibitory GABAergic (GABA) projections, respectively. There are three basic pathways of BG circuit: *direct* (purple), *indirect* (yellow) and *hyperdirect* (blue) pathways.

B) Cortically induced early and late excitations are mediated by the *hyperdirect* and *indirect* pathways, respectively.

Acknowledgments

The dissertation is a part of the requirements for receiving the doctor's degree, conferred by SOKENDAI. I would like to express my gratitude to Prof. Atsushi Nambu, Dr. Nobuhiko Hatanaka and Dr. Satomi Chiken for the help with the experimental model, the conductance of the research, critical discussions and encouragements for this research. I would like to thank Prof. Hitoshi Kita for help with the conductance of the experiments. I would like to appreciate Hitomi Isogai for help with monkey care and Shigeki Sato for technical assistance.

Finally, I would like to thank my parents, housemate, friends and all members of Prof. Nambu's laboratory in NIPS: Hiromi Sano, Dwi Wahyu Indriani, Taku Hasegawa, Daisuke Koketsu, Takuma Nishijo, Satomi Kikuta, Woranan Wongmassang, Pimpimon Nondhalee, Noriko Suzuki, Kanako Awamura, Kana Miyamoto and Tomomi Sugiyama for the support and encouragement for this research.